Coordination Chemistry Reviews 255 (2011) 664–677

Contents lists available at ScienceDirect

Coordination Chemistry Reviews

journal homepage: www.elsevier.com/locate/ccr

Review

Protein dynamics and function: Making new strides with an old warhorse, the alkaline conformational transition of cytochrome *c*

Melisa M. Cherney, Bruce E. Bowler*

Department of Chemistry and Biochemistry, Biochemistry Program and Center for Biomolecular Structure and Dynamics, The University of Montana, Missoula, MT 59812, United States

Contents

ARTICLE INFO

Article history:
Received 3 July 2010
Accepted 25 September 2010
Available online 7 October 2010

Keywords:
Cytochrome *c*
Alkaline transition
Gated electron transfer
Protein dynamics
Ligand switch

ABSTRACT

Protein dynamics is intimately linked to function. In metalloproteins, dynamics are often coupled to redox activity, ligand binding and enzyme function. We provide a concise overview of the field and then focus on the use of the alkaline conformer of cytochrome *c* as a model system to probe the factors that control the conformational dynamics of proteins in general and metalloproteins in particular. We consider the effects of ligands on metal-mediated dynamics, the interplay between intrinsic metal-ligand dynamics and barriers imposed by the protein scaffold itself, and the effects of local and overall protein stability on dynamics. Discussed within are the collected results from equilibrium thermodynamic methods, pH jump kinetics and conformationally gated redox reactions between small inorganic reagents and metalloproteins used as a means to probe conformational switching in metalloproteins.

Abbreviations[1]: a_6Ru^{2+}, hexaammineruthenium(II) chloride; CD, circular dichroism; Cyt*c*, cytochrome *c*; ET, electron transfer; FTIR, Fourier transform infrared spectroscopy; gdnHCl, guanidine hydrochloride; HX, hydrogen–deuterium exchange; K_a, association constant; k_b, backwards rate constant; k_{ET}, electron transfer rate constant; k_f, forward rate constant; k_{obs}, observed rate constant; *m*-value, rate of change of free energy with respect to denaturant concentration ($\delta\Delta G_u/\delta C$) which is proportional to the change in solvent-accessible surface area when a protein unfolds; NHE, normal hydrogen electrode; pK_a, negative log of the acid dissociation constant; pK_{app}, apparent pK_a; ΔSASA, change in solvent-accessible surface area; WT, wild type.

* Corresponding author. Tel.: +1 406 243 6114; fax: +1 406 243 4227.
E-mail address: bruce.bowler@umontana.edu (B.E. Bowler).

[1] Mutations used as variant names are abbreviated using the one letter code for the wild type amino acid followed by the position number and the one letter code for the new amino acid.

0010-8545/$ – see front matter
doi:10.1016/j.ccr.2010.09.014

1. Introduction

The structure–function paradigm has dominated the field of Biochemistry going back to Emil Fisher's "Lock-and-key" model for enzyme function in the 1890s [1]. Proteins were viewed as essentially rigid molecules in which the shape was intricately sculpted to enable highly specific interactions with small molecules or other proteins, and in which functional groups were precisely oriented to carry out function. Over 60 years later, Koshland's "Induced-fit" model emerged [2], with the recognition that conformational changes could be used to control enzyme function, particularly with multi-substrate enzymes, so that catalysis occurred only under appropriate conditions. Detailed studies on multi-subunit proteins, such as the oxygen-transport heme protein hemoglobin [3], demonstrated that such conformational changes could exercise "allosteric" control over the binding properties or catalytic activity of proteins and enzymes. Allosteric conformational changes typically occur in response to binding of small molecule ligands, including protons (i.e., pH). Thus, changes in environment (the presence or absence of a ligand) allow proteins to respond in a conditional manner.

The theory that changes in protein conformation control protein function is now widely accepted and constitutes an essential feature in the regulation of biochemical systems. Covalent modification of proteins provides an important method for switching protein activity on and off. For example, kinases and phosphatases mediate one key switching mechanism by controlling the phosphorylation of specific tyrosine, serine and threonine side chains [4]. Acetylation of histone lysines regulates gene transcription by altering chromatin structure [5]. In fact, recent experiments indicate that lysine acetylation may be as general a mechanism as phosphorylation for controlling protein activity [6,7]. However, it has become increasingly apparent that conformational fluctuations, even in the absence of covalent modification, are evolutionary adaptations that allow proteins to sample alternate conformers essential for function [8–10]. In some cases, conformational fluctuations are mediated by proline isomerization, which acts like a true on/off switch on a timer [11]. Conformational fluctuations occurring on the microsecond to millisecond time scale involve distinct thermodynamic states separated by barriers several times the magnitude of kT and are referred to as tier 0 processes [10,12]. In the funneled energy landscape that describes protein folding, where folding paths descend from the many high-energy, unfolded states up along the rim of the funnel to the few low-energy, folded states at the bottom of the deep potential energy well [13], tier 0 processes correspond to transitions to and from shallow wells adjacent to the folded native state. Functionally, tier 0 processes allow for transient sampling of alternate conformers that may confer activity, essentially acting to gate activity. Tier 0 processes can be coupled to binding events which shift the conformational equilibrium, driving the protein ensemble towards the activated (or inactivated) structure [10,14]. For metalloproteins, binding events which create a conformational shift may alter the coordination sphere and/or redox potential of the metal center, either through a direct interaction with the metal center or through indirect contacts in the protein structure [15–20]. Therefore, the metal site can provide a means to follow the conformational dynamics spectroscopically, especially in proteins where the conformational gate controls an electron transfer reaction [18,20–26]. Biologically, conformationally gated electron transfer may prove to be an essential means of regulating protein function, including redox-dependent enzyme activity [19].

The subject for this review is a set of conformational fluctuations observed in mitochondrial cytochrome *c* (Cyt*c*), a particularly well-studied metalloprotein found in a wide variety of organisms. Mitochondrial Cyt*c* is part of the larger cytochrome *c* family of electron transport proteins, each containing one or more *c*-type hemes covalently attached to the protein via thioether bonds through cysteine residues [27]. Mitochondrial Cyt*c* exists as a soluble monomer of ~100 amino acids with single *c*-type heme [16,27] and is part of the mitochondrial electron transport chain, transferring an electron from the cytochrome bc_1 complex to cytochrome *c* oxidase [27,28]. Additionally, the release of Cyt*c* from the mitochondria initiates a signal cascade that causes apoptosis [29]. Of keen interest to our lab is the observation that Cyt*c* switches its distal heme ligand when exposed to high pH, opening the heme crevice and creating a structure known as the alkaline conformation [16,17]. The significance of the alkaline conformation is unknown; it appears to resemble a late intermediate along the folding pathway [30–36], but there have also been indications that the open heme crevice structure is important for the role of Cyt*c* in both the electron transport chain [37–40] and apoptosis [41]. Opening of the heme crevice may serve as a conformational gate that helps to regulate these processes, making the alkaline conformational transition an interesting proxy for study.

Numerous thermodynamic and kinetic methods have been used to study the alkaline conformational transition in Cyt*c* [16,17]. This review will focus on results obtained using variants of yeast iso-1-Cyt*c* specifically designed to affect the alkaline conformational transition based on both the published structures of the native [42] and alkaline states [40], and knowledge of the folding substructures in Cyt*c* [32,33]. In addition to common equilibrium thermodynamic techniques including temperature- and denaturant-dependent unfolding and pH titration, the results of kinetic techniques will also be discussed, including pH jump stopped-flow mixing experiments and electron transfer studies conducted with a small inorganic reagent. We will present these studies with the goal of providing a clearer understanding of the alkaline conformational transition and its possible biological role, as well as the mechanisms by which the conformational gate could be tuned, were Cyt*c* to be used in the creation of protein-based molecular electronics devices [43–45].

2. Design of *c*-type cytochromes with alternate conformers

2.1. Cooperative units within cytochrome c

The unfolding of Cyt*c* from horse heart has been extensively studied using hydrogen–deuterium exchange (HX) methods [32,33,46–48]. In this method, the HX rate constants for the amide NH's of peptide bonds, k_{obs}, are measured and compared to the intrinsic rate constants of exchange, k_{int}, in disordered peptides [49]. HX data are interpreted according to the mechanism outlined in Eq. (1), where the Closed form is the native folded structure and the Open form is a state

$$\text{Closed} \underset{k_{cl}}{\overset{k_{op}}{\rightleftharpoons}} \text{Open} \xrightarrow{k_{int}} \text{Exchanged} \tag{1}$$

which allows the amide NH to exchange with solvent. The Open form can be a fully or partially unfolded form of the protein. This mechanism yields Eq. (2) for k_{obs}. For stable proteins under acid to neutral pH conditions, normally $k_{cl} \gg k_{int}$ (EX2 conditions) and thus Eq. (2) reduces to the form given in Eq. (3). The HX method has allowed the relative stabilities of different parts

$$k_{obs} = \frac{k_{op}k_{int}}{k_{cl} + k_{int}} \tag{2}$$

$$k_{obs} = \frac{k_{op}}{k_{cl}}k_{int} = K_{op}k_{int} \tag{3}$$

(substructures or foldons) of Cyt*c* to be determined [32,33]. These foldon units mapped onto the structure of yeast iso-1-Cyt*c* [42] are shown in Fig. 1. From least to most stable, these substructures are

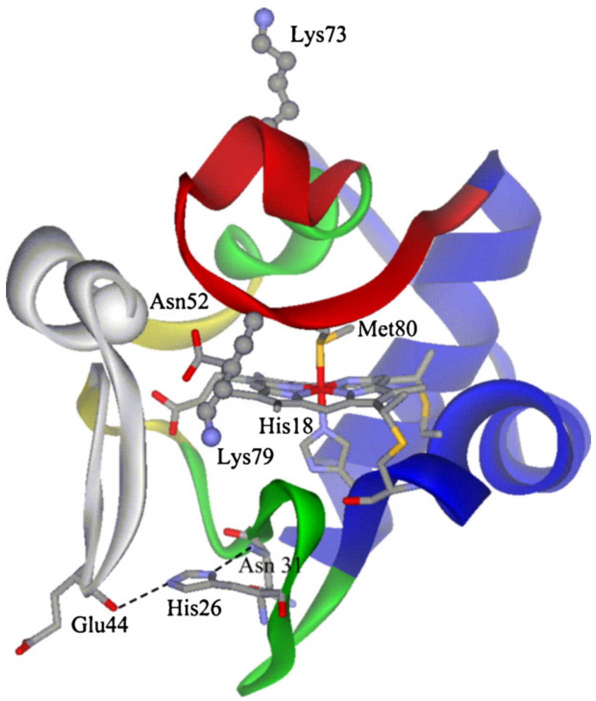

Fig. 1. Ribbon diagram of yeast iso-1-Cyt*c* in the ferric state (pdb code: 2ycc, [42], rendered with DS ViewerPro 5.0) with the foldons determined for horse Cyt*c* [32,33] mapped onto the structure. From least to most stable, these are the Infrared (gray), Red, Yellow, Green and Blue foldons. Shown as stick models colored by element are the heme; Cys14 and Cys17, which covalently attach the heme to the polypeptide; His18 and Met80, the heme axial ligands; and Glu44, His26 and Asn31, side chains involved in an inter-foldon hydrogen bond. The position of Asn52, which is mutated to glycine and other residues in variants discussed in this article, is shown as a gray sphere in the Infrared foldon. The lysines in the Red foldon which displace Met80 in the alkaline conformer of iso-1-Cyt*c* are shown as ball and stick models colored by element.

the Ω-loop that runs from residues 40 to 57 (Infrared foldon, gray in Fig. 1), the Ω-loop that runs from residues 71 to 85 (Red foldon), the short β-sheet which includes residues 37–39 and 58–61 (Yellow foldon), the 60's helix and the Ω-loop running from residues 20 to 36 (Green foldon) and the N- and C-terminal helices (Blue foldon).

Typically, HX measurements are done as a function of the concentration of a denaturant such as guanidine hydrochloride (gdnHCl). Protein stability varies linearly with denaturant concentration [50], as described in Eq. (4), where ΔG_u is the free energy of unfolding, $\Delta G_u{}^{o\prime}(H_2O)$

$$\Delta G_u = \Delta G_u{}^{o\prime}(H_2O) - mC \tag{4}$$

is the free energy of unfolding extrapolated to zero denaturant concentration and the *m*-value is the rate of change of free energy with respect to denaturant concentration, *C*. Theoretical [51] and empirical [52] studies indicate that the *m*-value is proportional to the change in solvent-accessible surface area (ΔSASA) when a protein unfolds. Thus, the denaturant dependence of ΔG_{op} ($=-RT\ln K_{op}$) from HX data provides insight into the size of a foldon. The *m*-value for the foldons of Cyt*c* increases progressively with foldon stability [33,53] (Fig. 2), which suggests that the foldons unfold sequentially, not independently. Sequential unfolding has been confirmed in "stability-labeling" studies which show that mutations that alter the stability of one foldon only affect the stability of more stable foldons, not less stable foldons [53–58]. In fact, the funneled energy landscape calculated for horse Cyt*c* is largely consistent with the sequential unfolding route observed with HX data [59]. However, the most recent HX studies indicate that branching is possible in the sequential folding/unfolding pathway of Cyt*c* [60]. There is also evidence for early collapsed intermediates and parallel pathways in the folding of both mitochondrial and bacterial cytochromes *c* [61–64]. Thus, it should be kept in mind that there are complexities in the folding/unfolding of Cyt*c* beyond the apparent simplicity of the sequential unfolding model based on the relative stabilities of the foldons of Cyt*c*.

Yeast iso-1-Cyt*c* is considerably less stable than horse Cyt*c* [58,65]. Limited proteolysis studies show that the least stable foldon is the same for both proteins [58] and also indicate that the relative foldon energies of the yeast protein are considerably compressed relative to the horse protein (Fig. 2). A similar compression of foldon energies is also observed for *Pseudomonas aeruginosa* cytochrome c_{551} [66], in which the global stability is intermediate to that of the horse and yeast proteins. As discussed below, we take advantage of the lower stability of the foldons in iso-1-Cyt*c* to stabilize alternate conformers using mutagenesis and heme ligand exchange reactions.

2.2. The alkaline conformational transition of cytochrome c

The alkaline conformational transition of Cyt*c* [16,17] is a long studied conformational change that occurs spontaneously between pH 8.5 and 11 in naturally occurring mitochondrial cytochromes *c* [16,67]. In yeast iso-1-Cyt*c*, site-directed mutagenesis studies have definitively shown that Lys73 and Lys79 in the Red foldon (Fig. 1) replace the native state Met80-Fe(III)heme ligand at elevated pH, creating the alkaline conformer [68,69]. When iso-1-Cyt*c* is recombinantly expressed in *Escherichia coli*, Lys72 is not trimethylated and can also act as a ligand in the alkaline state [70]. In horse Cyt*c*, Lys79 is the dominant ligand in the alkaline conformer, and Lys73 also contributes, but Lys72 plays only a minimal role as a heme ligand [71]. A variant of horse Cyt*c* in which Lys72, 73 and 79 were mutated appears to be able to use the N-terminal amine as a heme ligand, although it is unclear what role the free N-terminus plays when the preferred alkaline state ligands are available [71].

The alkaline transition is often monitored at 695 nm, a weak absorbance band that is usually assigned to a *z*-polarized porphyrin-to-Fe(III) transition (i.e., d_{z^2}, d_{xz} or d_{yz}) or a p(S)-to-d_π(Fe(III)) transition [16,72,73]. Thus, the 695 nm absorbance is sensitive to the axial ligand and loss of the Met80 ligand is normally associated with loss of this band [16]. The alkaline transition also can be observed at 398 nm in the intense heme Soret band [68]. pH titration data at either of these wavelengths is consistent with the alkaline transition involving release of a single proton. Therefore, the midpoint of the alkaline transition is usually reported as an apparent pK_a, pK_{app}.

The alkaline conformational transition requires a significant rearrangement of the Cyt*c* protein structure, particularly when Lys73 is the ligand in the alkaline conformer. The extent of this rearrangement has been revealed by NMR structural methods [40] (Fig. 3), making it clear that the primary structural perturbation involves the Red foldon. HX studies confirm the linkage between the Red foldon and the alkaline transition [31]; we review further thermodynamic evidence supporting this linkage in Section 3. Given the significant structural perturbation involved, changes in the conformational free energy of the Red foldon caused by mutations to Cyt*c* will have an important impact on the pK_{app} of this transition. Thus, the conformational free energy of the Red foldon must be kept in mind when interpreting the effects of mutations in terms of the mechanism of the alkaline transition of Cyt*c*.

The observed rate of the alkaline conformational transition may be limited by the dissociation rate of the native Met80 ligand and the subsequent opening of the heme crevice, rather than the binding rate of the alkaline state ligand. The rate of heme crevice opening, which predominantly consists of structural changes in the

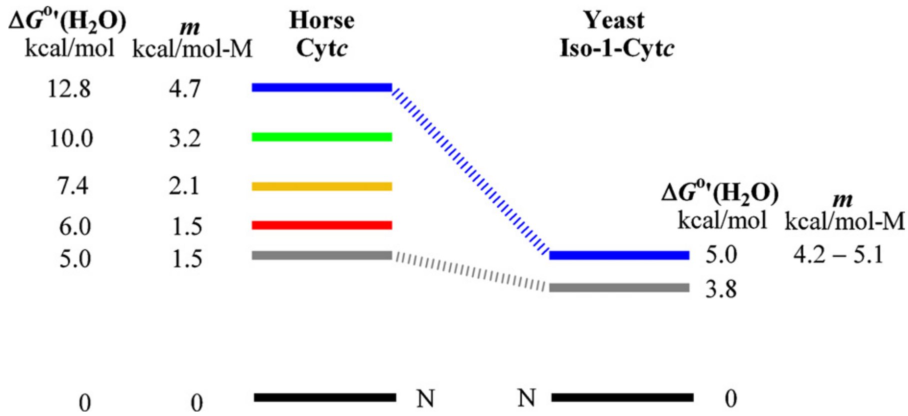

Fig. 2. Energy level diagrams for unfolding of the foldons of horse Cyt*c* and yeast iso-1-Cyt*c*. Free energies of unfolding, $\Delta G_u{}^{o\prime}(H_2O)$, and *m*-values are from refs. [33,53,55] for horse Cyt*c* and from ref. [58] for yeast iso-1-Cyt*c*. Color-coding is as in Fig. 1. N stands for the "native" fully folded structure.

Red foldon loop, constrains the maximum rate of exogenous ligand binding to the heme ($k \sim 30$–$60\,s^{-1}$) [74]. Furthermore, the similarity in horse Cyt*c* between the unfolding rate of the Red foldon measured by HX ($9 \pm 2\,s^{-1}$) and the limiting rate of the ligand switch during the alkaline conformational transition (7.5–$10.8\,s^{-1}$) suggests that it is the rate of Red substructure unfolding, including Met80 dissociation, that controls the rate of the alkaline transition [31]. Thus, mutations that affect the unfolding of the Red substructure would be expected to perturb the kinetics of the alkaline conformational transition.

2.3. Exploiting ligand exchange reactions to drive conformational changes

The stability of the Met-Fe(III)heme bond is relatively modest. The association constant, K_a, of the thioether of methionine for

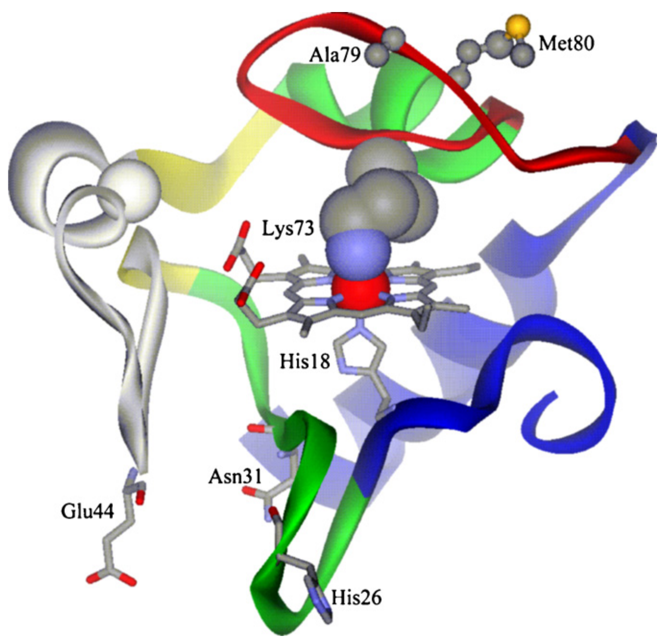

Fig. 3. Structure of the Lys73-heme alkaline conformer of the K79A variant of iso-1-Cyt*c* (pdb code: 1LMS, [40], rendered with DS ViewerPro 5.0). The foldons determined for horse Cyt*c* are mapped onto the structure as in Fig. 1. The heme and all visible amino acid side chains are colored by element. The heme is shown as a stick model, Lys73 and the iron of the heme are shown as space-filling models, Met80 and Ala79 are shown as ball and stick models, and His26, Asn31 and Glu44 at the base of the Green and Infrared (shown in gray) Ω-loops are shown as stick models. The structural data suggest that the hydrogen bonds that bridge between the side chain of His26 and the Infrared and Green foldons in the native structure are disrupted in the Lys73 alkaline conformer.

Fe(III)heme microperoxidase fragments of horse Cyt*c* has been estimated at ~3, whereas the K_a for imidazole (Im) is near 10^4 [54,75]. Thus, a Met-Fe(III)heme to His-Fe(III)heme ligand exchange reaction at 25 °C should provide ~5 kcal/mol ($RT\ln[K_a(\mathrm{Im})/K_a(\mathrm{Met})]$), making the ligand exchange reaction adequate to disrupt the Red foldon and stabilize the His-heme conformer near physiological pH, particularly for the less stable yeast iso-1-Cyt*c* (Fig. 2).

We have used this design principle to create variants of iso-1-Cyt*c* with histidines in the Ω-loop corresponding to the Red foldon, which have well-defined tier 0 conformational transitions. Due to the lower pK_a of histidine (~6.5) compared to lysine (~10.5), variants in which the lysines at positions 73 and 79 were replaced with histidine (K73H[1] and K79H variants, respectively) produce cytochromes *c* with His-heme conformers similar in stability to the native (Met80-heme) state near pH 7.5 [34–36,76,77]. Although the conformational transition to the His-heme state occurs near neutral pH, it is still referred to as the alkaline conformational transition (creating an alkaline conformer), since the conformational transition and structure is expected to be very similar between the His-heme and the Lys-heme conformers. We have used the lysine-to-histidine variants as a model system to probe the factors that modulate the thermodynamics and kinetics of tier 0 conformational transitions. We note that an F82H variant of iso-1-Cyt*c* produces exclusively bis(His) axial heme ligation in the Fe(III) state at pH 7 [78]. Thus, histidines in the Red foldon loop tend to displace Met80 at neutral pH. However, the dominance of the conformer with bis(His) axial ligation in the F82H variant of iso-1-Cyt*c* makes it a less convenient model for studying a tier 0 conformational transition [79].

3. Equilibrium thermodynamics of model tier 0 conformational transitions

3.1. Using denaturant unfolding to detect alternate conformers

In Section 2.1, we noted that the *m*-value ($\delta G_u/\delta C$) derived from denaturant unfolding of a protein is proportional to the change in solvent-accessible surface area when a protein unfolds (i.e., $m \propto \Delta$SASA). Thus, denaturant unfolding can provide insight into the amount of structure disrupted during the unfolding of a protein. When Lys73 of iso-1-Cyt*c* is replaced with histidine (K73H variant), the *m*-value obtained from gdnHCl unfolding at pH 7.5, monitored as loss of δ-helix structure by circular dichroism (CD) spectroscopy, is ~25% lower than that observed for wild type (WT) iso-1-Cyt*c* (inset Fig. 4) [34]. When gdnHCl unfolding is monitored at 695 nm (loss of heme-Met80 ligation) a much broader transition is observed, which is almost complete before CD moni-

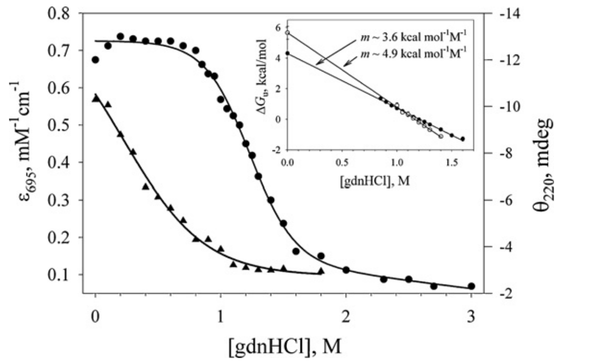

Fig. 4. Plots of extinction coefficient at 695 nm, ε_{695} (▲), and ellipticity at 220 nm, θ_{220} (●), versus gdnHCl concentration for the K73H variant of iso-1-Cyt*c* at pH 7.5 and 25 °C. Inset shows the free energy of unfolding, ΔG_u, versus gdnHCl concentration for the K73H variant (●) derived from the θ_{220} versus gdnHCl data. ΔG_u versus gdnHCl concentration for WT iso-1-Cyt*c* (○) is shown for comparison in the inset. The ΔG_u versus gdnHCl data were fit by Eq. (4) and the *m*-values are displayed on the graph. The *y*-intercept of the WT and K73H plots in the inset are shown as a visual aide; they are not actual data points.

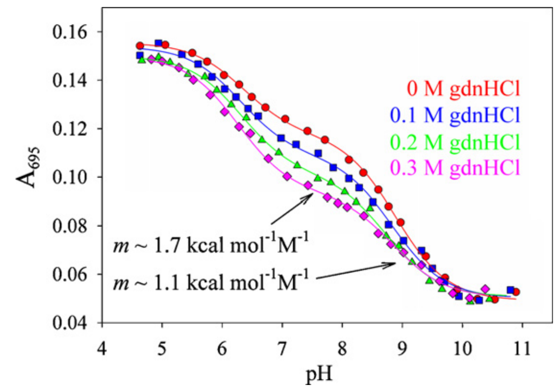

Fig. 5. Plot of absorbance at 695 nm, A_{695}, versus pH for K73H iso-1-Cyt*c* at different concentrations of gdnHCl. Data were collected in 0.1 M NaCl at 25 °C at protein concentrations near 200 μM, with 0 (red), 0.1 (blue), 0.2 (green) or 0.3 (pink) M gdnHCl added. The solid curves are fits of the data to the equilibrium model described in ref [36]. The unusual biphasic nature of the pH dependence of A_{695} results because the His73-heme conformer forms at lower pH, but reaches a limiting equilibrium constant with the Met80-heme conformer of ~1 around pH 7.5 when His73 is fully deprotonated (leveling out in the plot between pH 7 and 8). The loss of the Met80-heme conformer is then brought to completion by formation of the Lys79-heme conformer above pH 8. The gdnHCl *m*-values for the His73 and Lys79 heme-binding equilibria are shown. Adapted with permission from C.J. Nelson, B.E. Bowler, Biochemistry, 39 (2000) 13584–13594. Copyright 2000 American Chemical Society.

tored unfolding begins (Fig. 4). These data are consistent with the K73H protein forming an alternate conformer where His73 displaces Met80 before global loss of structure occurs. Interestingly, as pH is decreased toward pH 5, which will disfavor His73-heme ligation, the gdnHCl *m*-values for CD monitored unfolding for WT iso-1-Cyt*c* and the K73H variant approach each other [35]. NMR studies on the denaturant unfolding of horse Cyt*c* at neutral pH show partial population of a Lys-heme conformer (~15% in 7 M urea near the midpoint for global loss of structure) [80,81]. This conformer likely involves the alkaline state ligands and disruption of the Red foldon. The Lys-heme conformer is only significantly populated when the fully unfolded form is also populated. By contrast, the Met80-heme and His73-heme conformers of the K73H iso-1-Cyt*c* variant are both significantly populated near neutral pH in the absence of fully unfolded protein (Fig. 4). Thus, the K73H variant and related variants have allowed careful analysis of a tier 0 conformational transition.

3.2. pH and denaturant dependence of a tier 0 conformational transition

Studies on the pH dependence of Met80-heme ligation with the K73H variant of iso-1-Cyt*c* revealed that the native Met80-heme form is the sole conformer at pH 5. Near pH 7.5, the equilibrium constant between the His73-heme and Met80-heme conformers reaches a limit of ~1; at high pH the Lys79-heme alkaline conformer forms [36]. The clean separation of these equilibria allowed straightforward evaluation of the gdnHCl *m*-value for the individual equilibria (Fig. 5). For the K73H variant, the *m*-value is 1.67 ± 0.08 kcal mol^{-1} M^{-1} for formation of the His73-heme conformer and 1.1 ± 0.2 kcal mol^{-1} M^{-1} for formation of the Lys79-heme alkaline conformer. Thus, ΔSASA is larger when His73 replaces Met80 than when Lys79 replaces Met80, as might be expected since the Lys79 amino acid is only one position removed from Met80 (Fig. 1). The *m*-value for formation of the His73-heme conformer is similar to the 1.5 kcal mol^{-1} M^{-1} observed for unfolding of the Red foldon (Fig. 2), consistent with the significant disruption of the Red foldon expected when this conformer forms (Fig. 3). It is also interesting to note that the *m*-value for CD-monitored unfolding of the K73H variant (~3.6 kcal mol^{-1} M^{-1}) and formation of the His73-heme conformer (~1.7 kcal mol^{-1} M^{-1}) add up to the *m*-value for CD-monitored unfolding of WT iso-1-Cyt*c* (~4.9 kcal mol^{-1} M^{-1}) [65,82], within error. This additivity is consistent with a well-separated sequential unfolding of the K73H variant, involving first the Red foldon and then the rest of the protein.

A series of stabilizing mutations were added to the K73H variant of iso-1-Cyt*c* at position 52 (see Fig. 1) in the least stable Infrared substructure [57]. The change in global stability imparted by these mutations was equal to the change in free energy between the Met80-heme and His73-heme conformers, consistent with sequential unfolding of substructures in Cyt*c*. Similar *m*-values for formation of the His73-heme conformer and the Lys79-heme alkaline conformer were observed for this set of variants as for the parent K73H variant of iso-1-Cyt*c*. Thus, the extent of structural disruption to the Red foldon in conformers of Cyt*c* with alternate heme ligation appears robust to mutation.

For a K73H/K79A iso-1-Cyt*c* variant [76], the equilibrium thermodynamics of formation for the His73-heme conformer are more favorable than for the K73H variant at 0.1 M NaCl, but similar at 0.5 M NaCl. These results suggest that an electrostatic interaction between Lys79 and heme propionate D (~4.8 Å, Fig. 1) stabilizes the Met80-heme conformer relative to the His73-heme conformer. Also, spectra of the K73H/K79A variant above pH 8 show an absorbance band growing in near 620 nm, suggestive of a high-spin heme forming when Lys79 is absent. Studies with a K79H variant of iso-1-Cyt*c* show that formation of the His79-heme conformer is more favorable than the His73-heme conformer, relative to the native Met80-heme conformer [77]. This is opposite to the relative stabilities of the Lys73 and Lys79 alkaline conformers [68]. Thus, the structures of Lys-heme and His-heme conformers may differ in detail. However, replacement of Lys79, which is tightly packed against the surface of the protein in the Met80-heme conformer [42], with His may destabilize the native conformational state. Although the protonated His79 side chain may be able to form an electrostatic interaction with the heme propionate D similar to Lys79, the histidine side chain is too short to also form hydrogen bonds with the hydroxyl group of Tyr46 and the backbone carbonyl of Ser47 [42].

Clearly, replacement of lysine with histidine in the Red foldon makes alternate heme ligation conformers accessible at neutral pH. Since the stability of conformers with alternate heme ligation depends on both the relative affinities of the competing

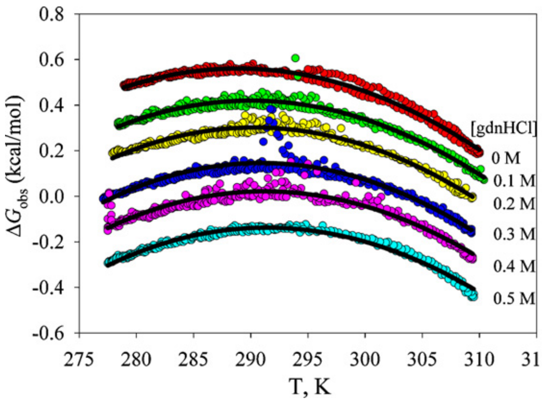

Fig. 6. Temperature dependence of the observed free energy, ΔG_{obs}, of the tier 0 conformational change from the Met80-heme to the His73-heme conformer of the K73H variant of iso-1-Cytc. The solid lines are fits of ΔG_{obs} as a function of temperature to Eq. (5) as described in ref. [30] at different gdnHCl concentrations. Adapted with permission from C.J. Nelson, M.J. LaConte, B.E. Bowler, J. Am. Chem. Soc., 123 (2001) 7453–7454. Copyright 2001 American Chemical Society.

heme ligands and the stability of the structure disrupted during ligand exchange, destabilization of the Red foldon or adjacent foldons can make Lys-heme alkaline conformers accessible at neutral pH, too. We find that $pK_{app} = 7.46 \pm 0.02$ for the Lys73-heme alkaline conformational transition of a N52G/K79A iso-1-Cyt*c* variant [83] with a destabilizing N52G mutation [84] in the Infrared foldon. P76G mutations in the Red foldon decrease the pK_{app} for the alkaline transition to 7.5 and 6.7 in horse Cyt*c* [71] and yeast iso-2-Cyt*c* [85], respectively. With iso-1-Cyt*c*, mutation of both Pro76 to Ala and Gly77 to Ala in the Red foldon decreases the pK_{app} for the alkaline transition to ~6.9 [86]. Mutation of Phe82 in the Red foldon also significantly favors the alkaline conformer [87]. Thus, the stability of the Infrared and Red foldons is an important component of the accessibility of Lys-heme alkaline conformers.

3.3. *Temperature dependence of a tier 0 conformational transition*

When a protein unfolds, buried hydrophobic residues are exposed to water. The hydration of these buried groups leads to an increase in the heat capacity of the system [88]. Under these conditions, the temperature dependence of the free energy of protein unfolding or of a protein conformational change, ΔG_c, is non-linear as given by Eq. (5), where ΔG_{max} is the free energy for

$$\Delta G_c = \Delta G_{max} + \Delta C_p[T - T_{max} - T\ \ln\left(\frac{T}{T_{max}}\right)] \quad (5)$$

the conformational change at T_{max}, the temperature of maximum stability, and ΔC_p is the change in the heat capacity of the system. We note that at T_{max}, ΔG_c is entirely enthalpic and the entropy change is zero; thus, the second term in Eq. (5) represents the temperature dependence of enthalpy and entropy due to ΔC_p [88]. The heat capacity change for protein unfolding, like denaturant *m*-values, is also proportional the ΔSASA [52]. Thus, the temperature dependence of stability can also provide insight into the extent of structural disruption in a tier 0 conformational change.

We followed the temperature dependence of ΔG_c at 695 nm (Met80-heme ligation) for the K73H variant of iso-1-Cyt*c* near neutral pH at several gdnHCl concentrations [30]. The ΔG_c for the tier 0 conformational change from the Met80-heme conformer to the His73-heme conformer shows the curved dependence expected for an equilibrium with a change in heat capacity (Fig. 6). The ΔC_p obtained from fitting the data to Eq. (5) is $0.48 \pm 0.03\ \text{kcal mol}^{-1}\ \text{K}^{-1}$ irrespective of gdnHCl concentration. A

$$\text{H}^+\text{Cyt}c \xrightleftharpoons{K_H} \text{Cyt}c + \text{H}^+ \underbrace{\xrightleftharpoons[k_b]{k_f}}_{K_C} \text{Cyt}c^* + \text{H}^+$$

Scheme 1. Simple mechanism for the formation of the alkaline state.

fit of ΔG_{max} versus gdnHCl concentration Eq. (4) at $T_{max} = 289 \pm 2$ K yields $m = 1.40 \pm 0.04\ \text{kcal mol}^{-1}\ \text{M}^{-1}$, similar to the value obtained from the pH and gdnHCl dependence of the formation of the His73-heme conformer with the K73H variant (Fig. 5) and the *m*-value for the Red foldon in horse Cyt*c* (Fig. 2). The ΔC_p for the full unfolding of iso-1-Cyt*c* is $1.40 \pm 0.06\ \text{kcal mol}^{-1}\ \text{K}^{-1}$ [89]. Both the *m*-value and the ΔC_p for the Met80-heme to His73-heme conformational change are about one third of the value for full unfolding of iso-1-Cyt*c*. Thus, this tier 0 conformational change exposes about one third of the buried surface area of the protein.

These well-characterized heme ligand exchange-driven tier 0 conformational transitions provide excellent substrates with which to study the factors that affect the dynamics of a tier 0 conformational transition. In the following sections, we demonstrate how standard pH jump mixing methods along with a novel electron transfer technique can be used to probe the dynamics of molecular switches that modulate protein function.

4. Dynamics of the conversion between conformers of cytochrome *c*

4.1. *Kinetic models for the alkaline conformational transition of cytochrome c*

According to the simplest model describing the alkaline conformational transition observed in Fe(III)Cyt*c*, the event takes place via two distinct steps: the deprotonation of a triggering group and the subsequent binding of a lysine ligand (Lys73 or Lys79 in yeast iso-1-Cyt*c*) to the heme in the place of the native Met80 ligand [90]. Scheme 1 illustrates this simple model, with H^+Cyt*c* and Cyt*c** representing the native and alkaline states, respectively. K_H is the ionization constant for the triggering group which initiates the conformational change. k_f and k_b are the forward and backward rate constants for the conformational change driven by the ligand switch and k_f/k_b is the equilibrium constant, K_C.

When inspecting Scheme 1, the simplest assignment for the triggering group which generates K_H is the lysine side chain [91,92], since the amine functionality will only bind to the heme iron in the deprotonated state. Thermodynamic and kinetic experiments have provided a pK_H that is near 11 and consistent with lysine deprotonation [31,68,87,90,93]. One study utilizing a set of lysine-to-alanine variants identified a strong correlation between the lowest theoretical pK_a calculated for the available lysine heme ligands and the pK_{app} observed during alkaline conformational transition experiments measured by cyclic voltammetry [91]. However, results obtained from experiments using chemically modified Cyt*c*, in which every lysine side chain was blocked by trifluoroacetylation, guanidination, amidation or maleylation, suggest that some other moiety may be the actual trigger which initiates the release of the native Met80 ligand and permits movement of a deprotonated lysine into position for heme binding [94,95]. In each chemically modified Cyt*c* species, the pK_{app} was only modestly perturbed, suggesting that the triggering group was largely unaffected by the chemical modification. Unfortunately, the chemical modifications may not have been structurally benign, since the heme in the alkaline conformation of trifluoroacetylated and guanidinated proteins was high-spin [94] and the pK_{app} of the maleylated protein was highly dependent on the ionic strength of the solution [95].

If the ionizable group that triggers the alkaline conformational transition in Cyt*c* is not the lysine heme ligand, the pK_a of the triggering group must still be near 11 to coincide with the measured pK_H. The similarity between the pK_H of the triggering group and the pK_a of the lysine ligand might then be theorized to have occurred by evolution, ensuring that deprotonation of both the triggering group and the alkaline state heme ligand is coordinated. Several non-lysine candidates have been proposed to serve as the triggering group [17], including a buried water molecule [96], which is adjacent to Met80; Tyr67, which hydrogen bonds to Met80 [97]; His18, the proximal heme ligand [98]; and one of the heme propionates, which has a pK_a shifted to >9 in the folded state of the protein [99,100]. The possible identity of the triggering group remains a topic for debate and will be further discussed in light of experiments using iso-1-Cyt*c* variants with alternate alkaline state heme ligands in Section 4.2. However, it should be noted that the alkaline conformational transition is (by most accounts, but see ref. [101]) thermodynamically a one proton process attributable to the lysine ligand, so if deprotonation of additional groups is required for the triggering event, those residues must be reprotonated after the ligand exchange is complete in order to maintain a net loss of only one proton. For example, the proposed mechanism in which the deprotonation of His18 acts as the trigger for the alkaline conformational transition employs a histidinate intermediate that rebinds a proton at the N_δ residue following the ligand exchange to the alkaline state [98]. In this model, reprotonation of the triggering group is necessary to match the observation that the heme iron in the alkaline conformation is ligated by two neutral nitrogen donors. Unfortunately, not all of the proposed non-lysine triggering groups would be likely to create a detectable spectroscopic signal upon reprotonation.

As might be expected, models for the alkaline conformational transition have been suggested which are variations on Scheme 1 [98,101–103]. When the alkaline conformational change is investigated by pH jump experiments to a final pH greater than 10, a second phase is seen in the kinetic data [31,93,102,104]. This second phase has been alternately explained as a parallel pathway to the alkaline conformation [93,102] or an unrelated deprotonation within the Infrared substructure [31]. Additionally, a high-spin, possibly five-coordinate, intermediate was identified by difference spectra [104] and resonance Raman [105], and was proposed to be part of a parallel pathway to the alkaline conformation which dominates at very high pH. It is unclear whether the high-spin intermediate and the second kinetic phase exist when the alkaline conformational transition occurs below pH 10, albeit at concentrations which are not detectable, or whether they only occur above pH 10. However, the pH jump kinetic experiments to be discussed in Section 4.2 were performed at or below pH 10 and the additional phase was not an issue.

Potential intermediates in the alkaline conformational transition have also been detected during equilibrium studies. pH titration experiments on Cyt*c* strategically labeled with deuterium and observed by FTIR revealed the formation of a species in which the native Met80-heme ligation was significantly perturbed, possibly even dissociated, although the switch to lysine–heme ligation had not yet occurred [101]. The formation of the intermediate occurred via a one proton process with a pK_a of 8.8, in line with the pK_{app} generally measured for the alkaline transition, while the subsequent transition to the Lys73- and Lys79-heme conformers required a second deprotonation and yielded a pK_a of ~10.2, leading the authors to suggest that formation of the intermediate species may be the true trigger which initiates the alkaline conformational transition. However, a related study using electronic absorption and CD spectroscopy to monitor the 695 nm band during the alkaline transition identified a native-like intermediate, which clearly retained the Met80-heme bond, if somewhat weakened, and only formed in buffer with a very low ionic strength and $H_2PO_4^-$ anion concentration [103]. Ionic strength, anion type, and binding anion concentration do modestly affect the Met80-heme environment [106], but no intermediate was visible in the salt and buffer concentrations more commonly used during pH titrations of Cyt*c* [103]. The intermediates detected by these two studies are qualitatively different. Also, pH titrations that monitor the heme methyl substituents by NMR spectroscopy only show clear evidence for the native state and lysine–heme bond alkaline conformers [36,68,107], implying that the chemical shifts of the methyl substituents in the intermediates detected by FTIR and at 695 nm would have to be similar to one of these end states. Additional investigation into these intermediate states is needed to better elucidate their role in the alkaline conformational transition of Cyt*c*.

4.2. Using alternate heme ligands to probe the mechanism of conformational change

In order to determine whether the ionizable triggering group observed in the alkaline conformational transition is in fact the alkaline state heme ligand, a series of lysine-to-histidine variants were examined in which the alkaline conformational transition is shifted to lower pH due to the lower pK_a of the new histidine heme ligand. Because only one of the two lysine residues in the Red foldon of iso-1-Cyt*c* (Lys73 or Lys79) was mutated to histidine, these variants actually contain two separate alkaline conformations: His-heme ligation near neutral pH and Lys-heme ligation at high pH. The presence of two conformational transitions predictably complicates the kinetic interpretation, so variants were also constructed in which the remaining lysine was mutated to an alanine.

pH jump mixing experiments conducted on the K73H variant of iso-1-Cyt*c* revealed that three separate ionizable groups participate in the triggering event for the His73-heme conformational transition, with the His73 heme ligand acting as the primary trigger [92] (Fig. 7). If deprotonation of the histidine side chain were the sole trigger for the conformational transition, a single pK_H of ~6.6 would be expected. Indeed, the amplitude attributable to histidine binding grows in with a pK_a of ~7, indicating that deprotonation of the histidine is the *thermodynamic* trigger and is necessary for heme binding. However, a fit to the k_{obs} rate data over both the downward and upward pH jumps yielded three distinct pK_a values for the His73-heme conformational transition (Table 1). Scheme 2 outlines the mechanism whereby three ionizable groups affect the kinetics of the alkaline conformational change. C(LH$^+$) and C(Fe-L) represent the native and alkaline states, respectively, where L is the heme ligand in the alkaline conformational state. LH$^+$/L, XH$^+$/X, and YH$^+$/Y represent the protonated/deprotonated forms of the ionizable groups (where X and Y are unidentified residues) and K_{HL}, K_{HX} and K_{HY} are the ionization constants for the ionizable groups. k_f and k_b are the forward and backward rate constants for the conformational change, numbered according to the path on which they occur. Since the model is drawn as a thermodynamic cycle, the ratio of k_f to k_b for each path should be equal to the equilibrium constant for the conformational change, K_C, as measured by equilibrium pH titration. While the heme ligand is the primary trigger that gates the conformational change, XH$^+$ and YH$^+$ can be viewed as auxiliary ionizations that change the stability of the transition state relative to the native and alkaline conformational states, thereby altering the magnitude of k_f and k_b for each path while K_C remains constant. Alternately, ionization of XH$^+$ and/or YH$^+$ could change the stability of both the native and alkaline states equally, while the transition state remains unaffected. Although the assumption that K_C remains constant over the entire pH range spanned by the three ionization events cannot be tested (since the primary trigger

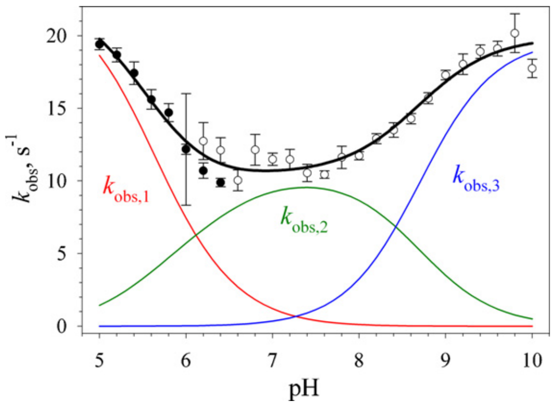

Fig. 7. Observed rate constant, k_{obs}, versus pH for the formation of the His73-heme conformer of K73H iso-1-Cyt*c* measured by pH jump stopped-flow mixing experiments conducted in 0.1 M NaCl at 25 °C. The closed and open circles represent the results for downward and upward pH jumps, respectively, and the black line is a fit to the combined pH jump data for the model in Scheme 2 [92]. The three pH-dependent components of k_{obs} created by the ionization of the XH^+, LH^+ and YH^+ triggering groups (Scheme 2) are plotted separately. Each component is the combined forward and backward rate constant for the conformational change over the relevant pH regime. The red line is $k_{obs,1}$ ($k_{f1} + k_{b1}$), the green line is $k_{obs,2}$ ($k_{f2} + k_{b2}$) and the blue line is $k_{obs,3}$ ($k_{f3} + k_{b3}$) (Scheme 2 and Table 1). The parameters from the fit to the data were used to generate each $k_{obs,x}$ plot. Adapted with permission from R.E. Martinez, B.E. Bowler, J. Am. Chem. Soc., 126 (2004) 6751–6758. Copyright 2004 American Chemical Society.

Table 1
Kinetic and thermodynamic parameters for the heme ligand exchange from Met80 to a histidine residue in yeast iso-1-Cyt*c*, as obtained from pH jump stopped-flow experiments at 25 °C.

Parameters	Variants[a]			
	K73H	K73H/K79A[b]	K73H/K79A[c]	K79H
k_{f1}, $s^{-1,d}$	11.4 ± 0.9	31 ± 26	7.2 ± 0.3	–
k_{b1}, s^{-1}	23 ± 2	25 ± 21	13.7 ± 0.5	–
k_{f2}, s^{-1}	3.5 ± 0.2	6.5 ± 0.3	3.7 ± 0.4	3.3 ± 0.2
k_{b2}, s^{-1}	7.0 ± 0.4	5.4 ± 0.3	7.0 ± 0.7	0.7 ± 0.2
k_{f3}, s^{-1}	6.6 ± 0.2	12.1 ± 0.5	6.4 ± 0.3	0.7 ± 0.1
k_{b3}, s^{-1}	13.2 ± 0.4	9.9 ± 0.4	12.0 ± 0.5	1.1 ± 0.1
pK_{HX}	5.6 ± 0.2	5 ± 1	6.4 ± 0.2	–
pK_{HL}	6.4 ± 0.5	6 ± 1	7.1 ± 0.5	6.75 ± 0.04
pK_{HY}	8.7 ± 0.2	8.8 ± 0.2	9.0 ± 0.2	9.21 ± 0.2
reference	[92]	[76]	[76]	[77]

[a] All variants contain a background C102S mutation to prevent disulfide formation and dimerization.
[b] Experiments were conducted in 100 mM NaCl.
[c] Experiments were conducted in 500 mM NaCl.
[d] The rate constant is constrained by K_C, which is assumed to be invariant with pH. k_{f1} is masked by K_{HL} as the pH drops below pK_{HL}; thus the assumption that K_C is invariant cannot be tested at low pH and may not be valid.

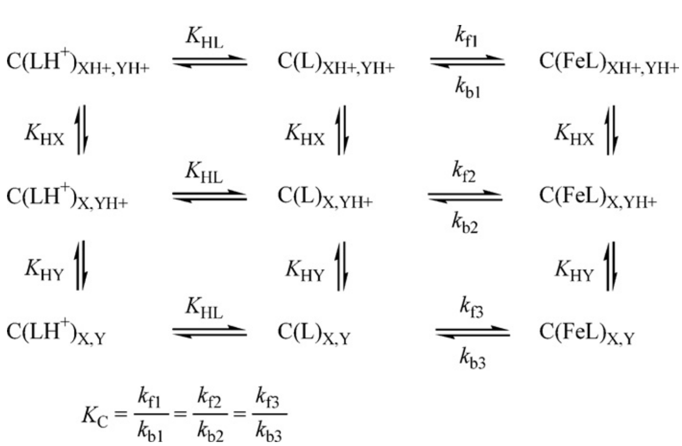

Scheme 2. Proposed three-trigger mechanism for the formation of the His73-heme conformational state.

masks k_{f1} at low pH), K_C did remain constant from about pH 8 to 10 in the K73H variant, where the amplitude of the His73 binding phase was unchanged once the ligand was fully deprotonated [92].

While pK_{HL} is easily assigned to the deprotonation of His73, the identity of the two auxiliary triggering groups is not obvious. His26 ($pK_a < 3.6$) was initially an attractive candidate for pK_{HX} due to its role in the His26/Glu44 hydrogen bond which stabilizes the native structure [108,109]. However, the disappearance of the pK_{HX} trigger in studies using a K79H variant (*vide infra*), where the His26/Glu44 hydrogen bond is still a factor, appear to rule out His26 as the triggering group [77]. Among the suggestions for the pK_{HY} triggering group are deprotonations that create an intermediate with either low-spin hydroxyl-heme [96] or high-spin Tyr67(phenolate)-heme ligation [97]. The hydroxyl-heme species normally begins to appear above pH 9, making it an unlikely explanation for pK_{HY}. Deprotonation of Tyr67 also seems an unlikely trigger, since no evidence for the formation of a high-spin intermediate was seen in the K73H pH jump data. Additionally, deprotonation of the Tyr67 would be expected to change the relative stabilities of the native and alkaline states as the side chain is ionized and moves from a buried to a solvent exposed position [40,42], whereas the almost constant amplitude attributable to histidine binding observed from pH 8 to 10 contradicts this theory. To date, the heme propionates seem the most likely candidates for the pK_{HX} and pK_{HY} triggering groups due to both their location and pK_a values, with one predicted to have a $pK_a < 4.5$ and the other a $pK_a > 9$ [16,99,100]. However, it is difficult to explain why deprotonation of the heme propionates would not have been apparent in the pH jump kinetics of previously examined Cyt*c* variants. By all appearances, WT Cyt*c* requires only a single ionization event to trigger the alkaline conformational transition. Several iso-1-Cyt*c* variants with mutations at Phe82 displayed significantly depressed pK_{app} values while the pK_C remained relatively unchanged, with pK_H values for the triggering group resembling pK_{HY} for the K73H variant [87]. However, the authors did not report any indication of additional ionization events in the data and there is no definitive evidence that the unusual decrease in the pK_H of the triggering ionization is related to the YH^+ ionization. Overall, there is no strong evidence that the auxiliary ionization triggers observed with the K73H variant affect the kinetics of the alkaline conformational transition in WT Cyt*c*. Therefore, the identities of the auxiliary triggering groups remain a topic for speculation.

Multiple ionizations were also apparent in the triggering events for the Lys-heme alkaline conformational transition and in a probable proline isomerization step seen in the kinetics of the K73H variant [92]. Although fitting the rate data for these minor phases was considerably more difficult, multiple pK_a's were tentatively identified in each transition. At least two triggering groups are involved in the alkaline conformational change from the native to the Lys79-heme state, with pK_a's of 7.0 ± 0.3 and 9.8 ± 0.4, roughly resembling those for the deprotonation of His73 and Lys79 (or possibly the YH^+ triggering group), respectively. The putative cis/trans Pro76 isomerization phase was assigned based on the rate of the transition [110], its relative amplitude when starting from either the native or alkaline states, and the work on a Pro76 to Gly mutant of iso-2-cytochrome *c* in which a slow folding phase seen in the WT protein was eliminated [111,112]. Proline isomerization is only seen in the K73H variant once the protein leaves the native state, requiring at least two ionization events with pK_a values of ~5.6 and 8.8 ± 0.2, in close agreement with the pK_{HX} and pK_{HY} observed for the His73-heme transition [92].

Further pH jump experiments using a K73H/K79A variant of iso-1-Cyt*c* verified that three separate ionizable groups control the Met80 to His73 heme ligand exchange and the conformational transition. As previously mentioned in Section 3.2, the K73H/K79A variant displayed salt-dependent properties and behaved thermodynamically and kinetically similar to the K73H variant only in 5 times the normal NaCl concentration [76], which was presumably necessary to stabilize the native conformation by replacing an electrostatic interaction that would have occurred between the Lys79 ε-NH_3^+ and the heme propionate D group [42,68]. The pK_{HX}, pK_{HL} and pK_{HY} values (Table 1) reported for the His73-heme conformational transition of the K73H/K79A variant in 500 mM NaCl were slightly higher than those measured for the K73H variant, albeit mostly within error. This difference could be explained by the elevated salt concentration and/or the Ala79 mutation, the latter of which may disrupt the buried hydrogen bonding network. While the K73H/K79A variant clearly lacks a Lys-heme alkaline conformer, it does produce the minor slow phase previously attributed to Pro76 isomerization. Similar to the K73H variant, the putative proline isomerization phase observed in the K73H/K79A variant requires deprotonation of at least two triggering groups, with pK_a values near 6 and 9.

It is not surprising that the transition from the native state to either the Lys-heme or His-heme conformational states differs to some degree, given the substantial difference in pK_a and heme binding affinity of the two alkaline state ligands. However, the disparity between the His73-heme and His79-heme conformational transitions illustrates the importance that sequence position plays, even when considering the largely flexible Red foldon. The His79 heme ligand in the K79H variant of iso-1-Cyt*c* might be expected to have approximately the same pK_a and heme binding affinity as the His73 ligand, and bind through a similar triggering event. Instead, the transition to the His79-heme conformer was triggered with only two ionizable groups, the ligand and the high pH trigger, corresponding to pK_{HL} and pK_{HY} [77] (Table 1). The conformational change in the K79H variant differs from the K73H variant due to the greater relative stability of the His79-heme conformer. Although the rate constant for histidine binding is approximately the same in both variants (~3.4 s^{-1}), the backwards rate constant is 10 times slower in the K79H variant, creating a larger population of the His79-ligated heme conformer around pH 7.5 and indicating a considerable stabilization of the His-heme conformational state relative to the native state in K79H iso-1-Cyt*c*. Additionally, the conformational transition of the K79H variant does not produce the slow, minor kinetic phase consistent with proline isomerization, suggesting that the replacement of Met80 with the adjacent His79 residue may cause a smaller structural rearrangement from the native form, preventing isomerization at the proline residue. This observation is consistent with *m*-values of 1.67 ± 0.08 and 1.0 ± 0.1 kcal mol^{-1} M^{-1} measured for the transition from the native to the His-heme state for the K73H [36] and K79H variants [77], respectively, indicating that the K79H variant undergoes a smaller change in structure during the conformational transition. Since the alkaline conformational transition is also dissimilar between the K79H and K73H/K79A variants, in both the number of auxiliary triggers and the relative stability of the His-heme form, destabilization of the native conformer due to the loss of the Lys79 side chain contacts cannot be the only reason for the unique behavior of the K79H variant. Compared to any of the His73 or His79 variants, the F82H variant of yeast iso-1-Cyt*c* demonstrates the strongest preference for its His-heme alkaline conformer ($k_f \approx 17$ s^{-1} and $k_b \approx 1$ s^{-1} [79]), even though the native Lys79 was not mutated and the histidine replaced a similar aromatic group also located on the Red foldon. Clearly, the placement of the alkaline state ligand on the Ω-loop of the Red foldon plays a significant role.

Overall, experiments with the lysine-to-histidine variants of iso-1-Cyt*c* have revealed several interesting properties of the alkaline conformational transition. First of all, the heme ligand in the alkaline state appears to be the primary triggering group which controls the conformational transition, since lowering the pK_a of the heme ligand causes an equivalent decrease in the pK_{app}, which would not be expected if some other group was the actual trigger. However, two auxiliary triggering groups affect the kinetics of the conformational transition in the K73H variants and have been tentatively identified as the heme propionates, although only one of the additional triggers was detected in the kinetics of the K79H variant and neither has been detected in the kinetics of the WT protein. The role and significance of the auxiliary triggering groups in the alkaline conformational transition is still poorly understood, but the solely kinetic effect observed for pK_{HX} and pK_{HY} could indicate that deprotonation at the additional sites alters the stability of the transition state relative to the native and His-heme conformers. Finally, when comparing the His73 and His79 variants, it is clear that the position of the histidine ligand within the flexible Red foldon has an important impact on the alkaline conformational transition.

5. Measurement of protein dynamics by an electron transfer method

5.1. Conformationally gated electron transfer theory

Electron transfer (ET) kinetics provide a particularly useful tool for studying those conformational changes which tune the ability of an active site to gain or lose an electron, especially when combined with a chemical oxidant or reductant whose concentration can be easily controlled. The square scheme mechanism (Fig. 8) outlines the two pathways available for a system that undergoes oxidation and reduction and has a preferred conformation for each redox state [113–117]. Cyt*c* and the chemical reductant hexaammineruthenium(II) chloride (a_6Ru^{2+}) are depicted, although the square scheme mechanism is applicable for many other systems [18,20,22,26,43,117–126]. When considering the reduction of Cyt*c* by a chemical reagent, the pathway taken will depend on the reduction potentials and relative stabilities of the intermediates, as well as the concentration and reduction potential of the chemical reagent used. For instance, if the reduction potential of an Fe(III)Cyt*c* variant in the alkaline conformation is accessible by the chemical reagent, reduction and subsequent rearrangement to the native conformation will occur by the stepwise process in Pathway A. However, if the reduction potential of the alkaline conformer is too low, Pathway B will be favored and the conformational change must occur before ET can be achieved. In this manner, the observed rate of reduction can be controlled by the dynamics of the conformational change. When the rate of the conformational change is significantly slower than the rate of ET, the system is described as undergoing conformationally gated ET. Since the reaction will only be gated in one direction (either reduction or oxidation), the conformational gate can act as either a molecular switch, which is kept off until just the right conditions are present, or as a valve for electrons that impedes deleterious backflow. It has been suggested that the alkaline conformation may resemble the structure of Fe(III)Cyt*c* when complexed with cytochrome *c* oxidase, its redox partner in the mitochondrial electron transport chain [37–40]. This theory is particularly attractive as it provides a means for unidirectional electron flow in the complex.

For a conformationally gated system in which there is an equilibrium between the two conformers in the original redox state, as represented by the left half of the square scheme for an Fe(III)Cyt*c* sample, the kinetic data will contain a phase for the ET reaction of each conformer with an amplitude that is proportional to the population of that conformer in the original sample. The component which is already in the correct conformation can undergo direct ET and the observed rate for the formation of the reduced species will be linearly dependent on the concentration of the reductant (Eq.

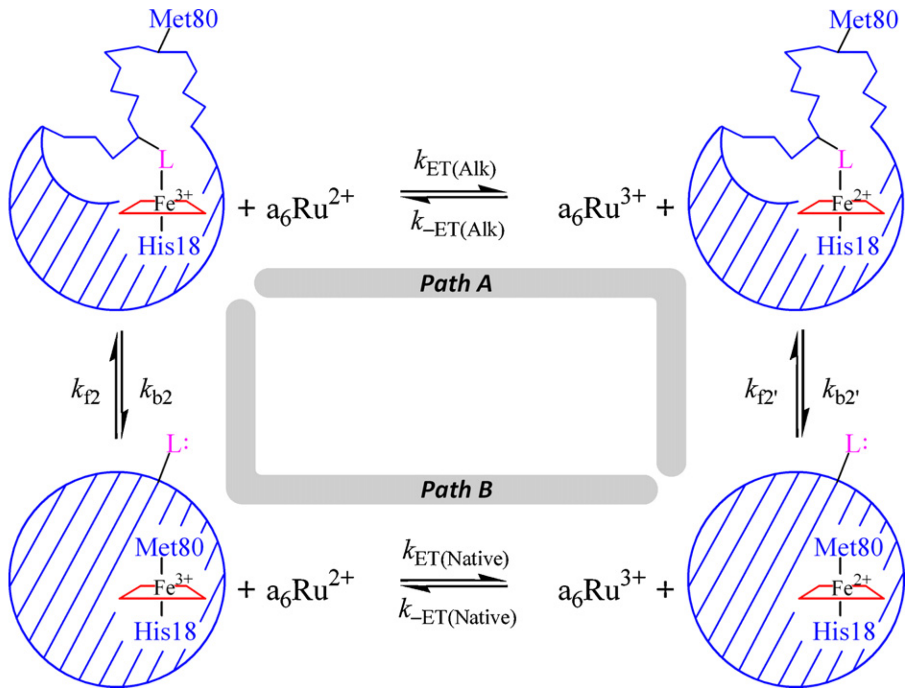

Fig. 8. Square scheme mechanism for conformationally gated ET in iso-1-Cyt*c*. The reaction between oxidized Cyt*c* and hexaammineruthenium(II) (a_6Ru^{2+}) is depicted at the top and bottom left, ultimately yielding reduced Cyt*c* and a_6Ru^{3+} at the bottom right. Pathway B is favored when Cyt*c* is reduced with a_6Ru^{2+}. The top row contains the oxidized and reduced alkaline conformer, with L representing a histidine or lysine heme ligand, depending on the variant. The bottom row contains the oxidized and reduced native conformer, with Met80-heme ligation. The horizontal reactions describe the ET equilibria; $k_{ET(Native)}/k_{-ET(Native)}$ and $k_{ET(Alk)}/k_{-ET(Alk)}$ are the forward/backward ET rate constants for the native and alkaline state ligand conformations. The vertical reactions describe the conformational equilibria between the alkaline and native ligation states; k_{f2}/k_{b2} and $k_{f2'}/k_{b2'}$ are the forward/backward rate constants for the ligand exchange in the oxidized and reduced heme states. The direction of k_{f2} and k_{b2} are assigned to match the convention used for the pH jump kinetic studies on the alkaline conformational transition of oxidized Cyt*c*. For ET experiments conducted at approximately neutral pH, the rate constants for the ligand exchange in Pathway B (the conformational gate) are equivalent to k_{f2} and k_{b2} measured by the pH jump kinetics reported in Table 1. For variants with auxiliary triggering groups affecting the alkaline conformational transition, the k_{f1}/k_{b1} and k_{f3}/k_{b3} rate constant pairs (from Scheme 2 and Table 1) describe the ligand exchange in the low and high pH regimes.

(6), inset to Fig. 9). However, the component of the sample that

$$k_{obs} = k_{ET} \cdot [\text{reductant}] \tag{6}$$

undergoes gated ET will display a more complicated relationship to the reductant concentration, as shown for the reduction of a Cyt*c* variant in Fig. 9. In this case, Pathway B is favored and the k_{obs} measured for gated ET depends on the forward and backward rate constants for the conformational change (k_{f2} and k_{b2}, in Scheme 2 at pH 7.5), as well as the k_{ET} and reductant concentration [117] Eq. (7).

$$k_{obs} = \frac{k_{ET} \cdot k_{b2} \cdot [\text{reductant}]}{k_{ET} \cdot [\text{reductant}] + k_{f2}} \tag{7}$$

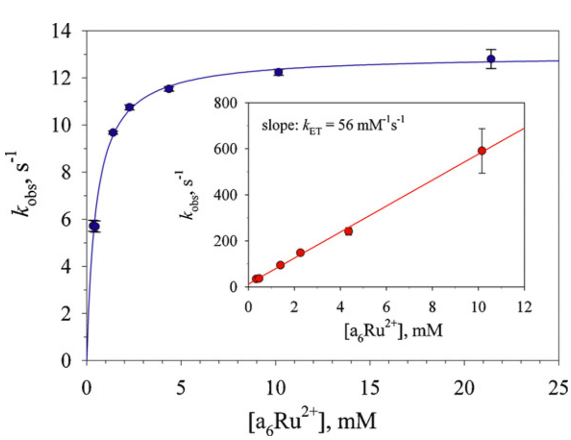

Fig. 9. Plot of the observed pseudo first-order rate constant, k_{obs}, versus a_6Ru^{2+} concentration for the reaction between the oxidized H26N/K73H variant of iso-1-Cyt*c* and a_6Ru^{2+}. The reduction of the His73-heme conformer proceeds via gated ET. The solid curve is a fit to the data using Eq. (7). The inset is a plot of k_{obs} versus a_6Ru^{2+} concentration for the direct reduction of the native conformer (Met80-heme ligation), with the data fit by Eq. (6). The experiments were conducted at 25 °C in pH 7.5 buffer containing 0.1 M NaCl [140]. Adapted with permission from S. Bandi, B.E. Bowler, J. Am. Chem. Soc., 130 (2008) 7540–7541. Copyright 2008 American Chemical Society.

When the reductant concentration is very high, Eq. (7) reduces to $k_{obs} = k_{b2}$ and the rate constant for gated ET plateaus. However, if k_{ET} for the reductant is much larger than the rate constant for switching the conformational gate to the ET inactive form (k_{f2}), Eq. (7) reduces to $k_{obs} = k_{b2}$ at every reductant concentration at which pseudo-first order kinetic data can be collected, and only the rate constant for switching the conformational gate to the ET active form (k_{b2}) can be directly measured. When k_{ET}[reductant] approaches the magnitude of k_{f2}, the reaction enters the coupled ET regime, and it becomes possible to evaluate k_{f2}. For example, in Fig. 9, when k_{obs} is at half the value of its final plateau, the reductant concentration can be used to calculate k_{f2}, since $k_{ET}[\text{reductant}] = k_{f2}$ when $k_{obs} = k_{b2}/2$. Careful consideration is required when choosing a reductant (or oxidant) for a conformationally gated system. The k_{ET} for the reagent must be both large enough that the process is truly gated by the conformational change and small enough that the rate constant for switching the conformational gate to the ET inactive form can still be evaluated.

5.2. An example of conformationally gated electron transfer with small inorganic complexes

The first well-characterized example of a system displaying the conformationally gated ET described by the square scheme mechanism was a series of Cu(II/I)-macrocyclic polythiaether complexes, for which the ET rate of the metal center differed depending on whether the measurement was taken during oxidation or reduction of the copper complex, even when the ET rate of the redox reagent used was taken into account [117,127–131]. Detailed kinetic analysis revealed that the oxidation reaction proceeded via a conformationally gated mechanism which controlled the observed rate of ET (Pathway A, starting from the bottom right of the square scheme). Macrocyclic ligands tailored to favor a more tetrahedral geometry, with a destabilized Cu(II) state, created complexes in which reduction became the conformationally gated process [132–134] (Pathway B, starting from the top left of the square scheme). Although it is possible that the square scheme applies to the redox couples of most metal complexes, the rate of conformational interconversion with even highly constrained ligands is likely too fast to be detectable by conventional kinetic methods.

5.3. Conformationally gated electron transfer using the alkaline conformer of cytochrome c

Conformationally gated ET can be observed in Cyt*c* when the alkaline conformation is reduced [23–25]. The native Met80-heme ligation of Cyt*c* has a reduction potential of about 290 mV (versus NHE) [68], which allows it to be reduced by even modestly powerful chemical reductants. However, the Lys-heme and His-heme alkaline conformational states have reduction potentials of about −205 and 0 mV (versus NHE), respectively [68,79,135,136]. If a reductant is chosen with an intermediate reduction potential (a_6Ru^{2+} is ~50 mV versus NHE, [137]), the alkaline state cannot be reduced directly, but will first have to undergo a ligand switch back to the native ligation state. This case corresponds to Pathway B on the square scheme mechanism, in which the conformational gate is essentially the alkaline conformational transition in reverse. Since the conformational change in Cyt*c* involves the exchange of a heme ligand, which can only occur via an S_N1 type reaction mechanism, the square scheme could be drawn to have an additional intermediate on each pathway to account for the five-coordinate heme species which must form at least transiently during a ligand switch. A high-spin species has been observed as a minor phase during pH jump experiments when the final pH is greater than 10 [102,104,105], and a long-lived high-spin intermediate is produced by a F82W variant of iso-1-Cyt*c* at mildly alkaline pH [97], but these species are more likely six-coordinate with an oxygen from Tyr67 or water in the distal heme binding site. No indication of an additional intermediate has been observed in the kinetic data of conformationally gated ET, suggesting that the five-coordinate species is present for too short a time to be detected.

In WT iso-1-Cyt*c*, the conformational gate created by Lys-heme ligation only occurs at relatively high pH (where lysine can be deprotonated) and exchanges slowly with the native Met80-heme ligation, such that conformationally gated ET occurs on a ~30 s time scale [23–25]. Depending on the pH, the ferric protein initially exists with a mixed equilibrium population of the Met80-heme and Lys73- or Lys79-heme alkaline states. While the alkaline state can only be reduced after undergoing the conformational change, the population already in the Met80-ligated state can be reduced directly, providing a measure of k_{ET} for the chemical reductant. When a_6Ru^{2+} was used as a reductant with the WT protein, the k_{ET} was measured at $48 \pm 4\,mM^{-1}\,s^{-1}$ [138]. In order to learn more about the kinetics of the conformational gate, and the alkaline conformational transition in general, a series of variants were constructed in which the dynamics or the pK_{app} of the alkaline transition were altered and the rate of heme reduction was measured as a function of the pH and a_6Ru^{2+} concentration.

Table 2
Kinetic parameters for the conformationally gated ET process in yeast iso-1-Cyt*c* using a_6Ru^{2+} as a reductant at pH 7.5 in 100 mM NaCl and at 25 °C.

Variant[a]	Rate constants			*Reference*
	k_{ET} ($mM^{-1}s^{-1}$)	k_{b2} (s^{-1})	k_{f2} (s^{-1})	
WT	48 ± 4	–	–	[138]
K73H	39 ± 5	6.9 ± 0.9[e]	–	[138]
K73H/K79A	133 ± 9[c]	5.09 ± 0.09[e]	–	[139]
N52G/K79A	160 ± 40[d]	0.056 ± 0.008[e]	–	[139]
K79H	84 ± 17	0.63 ± 0.02[e]	–	[77]
H26N/K73H[b]	56 ± 7	13.1 ± 0.2	28.1 ± 2.4	[140]

[a] All variants contain a background C102S mutation to prevent disulfide formation and dimerization.
[b] Variant contains 4 additional background mutations (T(-5)S, K(-2)L, H33N, and H39Q) and N-terminal acetylation.
[c] The reported k_{ET} value measured at pH 7.5 is likely somewhat low.
[d] Measured at pH 6.
[e] Average and standard deviation of the k_{obs} values reported for the slow phase at 1.25, 2.5 and 5.0 mM a_6Ru^{2+}.

5.4. Tuning a conformational gate using variants of cytochrome c

Unlike the WT protein, the K73H variant of iso-1-Cyt*c* can undergo the alkaline conformational transition near neutral pH due to the substantially lower pK_a of histidine [92,138]. Conformationally gated ET is observed for the K73H variant at physiologically relevant pH, and the histidine ligand has the further effect of altering the rate of the conformational gate. The greater lability of the histidine–heme bond accelerates the observed ET rate for the conformationally gated process to a 50–100 ms time scale, an increase of nearly 500-fold. Furthermore, the rate constant for conformational gating (k_{b2}, Table 2) is essentially the same as the rate constant for the His73-heme to Met80-heme ligand exchange measured by pH jump kinetics (k_{b2}, Table 1), confirming that the ligand switch back to the native state is the process which creates the conformational gate.

The rate of conformationally gated ET in iso-1-Cyt*c* can also be affected by mutations which alter the relative stabilities of the native and alkaline conformers. The measured rate constant for gated ET in the K73H/K79A variant [139] is ~30% smaller than that of the K73H variant. The Ala79 mutation used to simplify the ET kinetics by eliminating the Lys79-heme binding phase also affects the stability of the variant. Relative to K73H, the native state of the K73H/K79A variant is destabilized by ~0.4 kcal/mol when measured in typical buffer solution containing 100 mM NaCl [76], apparently due to the loss of electrostatic and hydrogen bonding contacts normally formed by Lys79 [42]. These contacts do not exist in the alkaline conformer [40], as the Red foldon containing position 79 is significantly perturbed, suggesting that the Ala79 mutation should not have a significant impact on the stability of the His73-heme conformer (Fig. 3). Global unfolding studies conducted at pH 7.5, when the protein is predominantly in the His73-heme state, indicate that the stability of the His-heme conformer for the K73H and K73H/K79A variants is equivalent [34,36,76]. Although the stability of the His-heme conformational state appears unaffected by the Ala79 mutation, the dynamics of the K73H/K79A conformational gate are altered in both directions, suggesting that the stabilities of both the native and transition states of the K73H/K79A variant have decreased relative to the K73H variant when considering experiments conducted in 0.1 M NaCl. The result of the Ala79 mutation is a variant in which the conformational gate has been modestly slowed, with agreement between measurement of k_{b2} by ET and pH jump kinetics (Tables 1 and 2), indicating that it is possible to use mutagenesis to fine turn the rate of gated ET in Cyt*c*.

Mutations outside of the flexible Red foldon loop that provides distal heme ligands can also have a profound effect on the conformational gate. Since the folding of substructures in Cyt*c* is sequential, destabilization of the least stable Infrared foldon will not only destabilize the Red foldon, but the entire native conformation [53–58]. The mutation of Asn52 to Gly in the Infrared foldon significantly decreases the global stability of iso-1-Cyt*c* [84]. An N52G/K79A variant of iso-1-Cyt*c* was constructed in which the Gly52 and Ala79 mutations disrupt the buried hydrogen bonding network of the native conformation to such an extent that the transition to the Lys73-heme alkaline conformational state is shifted down more than a pH unit, making the alkaline conformation accessible over the pH 6–8 range, despite a pK_H of ∼9.5 for the triggering ionization [83]. Although the conformational gate remains slow, operating on an approximately 15–20 s time scale [139], it now occurs at a potentially more useful, physiologically relevant pH.

Dramatic destabilization of Cyt*c*, necessarily affecting both the native and alkaline states, appears to lower the kinetic barrier between the conformations, increasing the rate of the conformational gate. The H26N/K73H variant of iso-1-Cyt*c* displays less than half the stability of the K73H variant and has a conformational ET gate that is twice as fast [140]. The radically destabilized H26N/K73H variant contains several mutations, including a His26 to Asn mutation that breaks up a vital hydrogen bond which bridges His26 of the Green foldon and Glu44 of the Infrared foldon [109] (Fig. 1) and is the primary cause of the decrease in global stability for the variant. Stopped-flow ET studies of the H26N/K73H variant revealed that the dynamics of the conformational gate were accelerated in both directions, presumably due to increased plasticity of the altered protein structure [140]. As the depth of the potential energy well describing the protein folding landscape was decreased in the less stable protein, so too were the transition barriers between the Met80 and His73 ligation states, creating the more rapid gate dynamics. In addition, both the k_{f2} and k_{b2} values for the H26N/K73H variant were large enough to be measured by reduction with the a_6Ru^{2+} reagent (Table 2). In all of the previously discussed variants, the plot of k_{obs} versus a_6Ru^{2+} concentration was flat, as the rate of reduction was too fast to permit direct determination of k_{f2} [77,138,139]. For the H26N/K73H variant, k_{obs} shows a hyperbolic dependence on the a_6Ru^{2+} concentration that can be fit by Eq. (7), providing a measure of k_{f2} (Fig. 9).

Changing the position of the histidine ligand on the Red foldon loop can also have a profound effect on the conformational gate, as shown by the K79H variant of iso-1-Cyt*c*. Although the Red foldon is quite flexible, moving the histidine ligand from the 73 to the 79 position slows the conformational gate almost 10-fold, in agreement with k_{b2} measured by pH jump kinetics [77] (Tables 1 and 2). Judging by the k_{f2} and k_{b2} values for the K73H, K73H/K79A and K79H variants, and the corresponding rate constants for the F82H variant [79], a change in the histidine position on the Red foldon Ω-loop significantly alters the relative stability of the native and His-heme states, regardless of any destabilizing mutations at the Lys79 position. While the shape of the Red foldon in the Lys73 alkaline conformer is significantly perturbed (Fig. 3), the structure of the alkaline conformer is clearly influenced by the position of the heme ligand along the Ω-loop, producing alkaline conformers with different stabilities.

Mutation of the Lys79 position in iso-1-Cyt*c* to either alanine or histidine revealed that the amount of positive charge surrounding the heme crevice affects the rate of direct electron transfer from a_6Ru^{2+}. Removal of the positive charge at position 79 by mutation to alanine increased the k_{ET} to approximately 150 mM^{-1} s^{-1} for the K73H/K79A and N52G/K79A variants [139], about 3–4 times faster than the k_{ET} measured for the WT protein [138]. Similarly, the His79 mutation acts like a partial removal of positive charge, possibly due to the lower pK_a of histidine, producing a k_{ET} for the K79H variant almost twice that of the WT protein [77]. For both small molecule redox reagents [141–148] and cytochrome *c* oxidase [149], the site

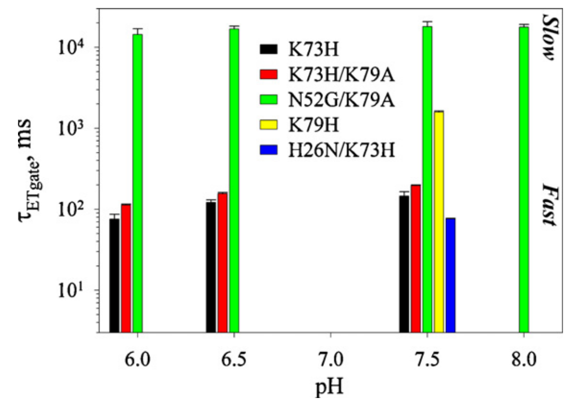

Fig. 10. Bar graph of the time constant ($\tau_{ET\,gate}$) for the ET gate of several yeast iso-1-Cyt*c* variants measured using a_6Ru^{2+} as a reductant over a range of pH values. $\tau_{ET\,gate}$ was calculated from k_{b2} (from Table 2 and references within), the rate constant for switching the conformational gate to the ET active form (Met80-heme ligation), using the equation $\tau = 1/k$. The slow and fast ET gate regimes are indicated at the side of the graph.

for ET occurs near the exposed heme edge in Cyt*c*. Overall, the surface surrounding the heme edge contains a disproportionate number of lysines and a high degree of positive charge, creating a molecular dipole moment [150]. Interactions with positively or negatively charged redox reagents or cytochrome *c* oxidase tend to occur in one of three loosely defined sites around the heme edge [141,146]. Blocking or altering the charges of the lysine residues at these three sites tends to increase the ET rate for cationic reagents and decrease the rate for anionic reagents [143–145], as might be expected if electrostatic interactions were the primary determinant. Although Lys79 does not fall into one of the defined sites, its side chain covers the heme edge, so its removal may provide a more optimal site for a_6Ru^{2+} binding during ET [42].

The rate of the conformational gate observed in iso-1-Cyt*c* can also be modified by pH. For variants in which k_{f2} is much smaller than the k_{ET} for a_6Ru^{2+}, and therefore could not to be measured, k_{b2} is the rate constant that limits the gated ET reaction. The effects of pH on the rate of the His-heme to Met80-heme ligand exchange can be viewed in Table 1, where k_{b1}, k_{b2} and k_{b3} represent the ligand exchange rate constants for the low, neutral and high pH regimes, respectively. As the pH increases from low to neutral and the XH^+ triggering group is deprotonated (Scheme 2), k_b decreases, indicating that the conformational gate should slow as the pH increases over this range. In fact, the rate of the conformational gate in the K73H and K73H/K79A variants does slow over the pH 6.0–7.5 range, as shown by the increasing time constant for the ET gate (Fig. 10). Thus, adjustment of pH provides another way to tune the dynamics of the conformational ET gate created by the alkaline conformational transition.

Tuning the conformationally gated ET behavior of Cyt*c* is possible through a number of different strategies. To shift the pH at which the conformational gate is effective, the most straightforward method is to replace the native alkaline state ligand(s) with a ligand that has a different pK_a, although the amino acid choice is fairly limited. Fortunately, even the pK_{app} for the transition to the Lys-heme conformer can be moved if the relative stabilities of the native and alkaline states are sufficiently perturbed. Mutations that preferentially affect the stability of only one of the two conformers (or the transition state) are the key to altering the dynamics of the conformational gate. They may be designed to act directly, by forming or eliminating contacts between the Red foldon and the rest of the protein, or indirectly, by making mutations that change the stability of the Infrared foldon and are communicated to the Red foldon due the sequential nature of substructure folding in Cyt*c*. Changes in the global stability of Cyt*c* can be used to adjust the kinetic barriers between the conformations, since the free energy landscape scales with the depth of the potential energy well. Even the position of the alkaline state ligand on the Red foldon affects the relative stability of the alkaline state. Adjusting factors such as the ionic strength, the pH and the concentration or identity of the reducing agent can also be used to alter the dynamics of conformationally gated ET. Combined, these factors have been used to produce Cyt*c* variants that range over more than 2 orders of magnitude in their rate of conformationally gated ET.

The combination of metal ions, ligand identity and local conformational stability have provided nature with a powerful set of tools for creating a wide range of conformationally gated ET rates, which in turn control many essential enzymatic reactions [19]. With Cyt*c* as a model system, we have shown that these factors can modulate the rate of gated ET from the 100 ms to the 10 s time scale (Fig. 10). Our work has focused on heme-mediated conformational dynamics. In copper proteins, ligand exchange provides for ET gating down to the microsecond time scale [18]. Thus, nature can control enzymatic mechanisms and metabolism as a whole from the microsecond to the second time scale by manipulating metal-mediated conformational gates that control electron flow.

6. Summary

The control of dynamics is an essential feature built into all proteins, especially those whose function requires a conformational change, such as during enzyme activity or allosteric regulation. As seen in the alkaline conformational transition in Cyt*c*, nature has developed a range of structural interactions between amino acid functional groups that allow protein dynamics to be tailored for specific functions and environmental conditions, such as the range of dynamics observed in enzymes from psychrophilic, mesophilic and thermophilic organisms [10,151,152]. Conformational gating is a crucial method for regulating protein activity, and it is increasingly being discovered as a method for controlling ET in redox-dependent enzymes. The ability to tune conformational gates through mutagenesis and solution conditions may also provide molecular switches that could be useful in the design of protein-based molecular electronics devices [43–45], especially for robust proteins like Cyt*c*.

Acknowledgements

The authors thank the National Science Foundation (NSF, Arlington, VA) for on-going support of this work, most recently through CHE-0910616. Congratulations, Harry, on your 75th birthday! We look forward to many more. No one else makes science fun the way you do!!!

References

[1] E. Fisher, Ber. Dt. Chem. Ges. 27 (1894) 2985.
[2] D.E. Koshland Jr., Cold Spring Harbor Symposia in Quantitative Biology, vol. 52, 1987, p. 1.
[3] E. Antonini, M. Brunori, Hemoglobin and Myoglobin in their Reactions with Ligands, North-Holland Pub. Co, Amsterdam, 1971.
[4] L.N. Johnson, D. Barford, Annu. Rev. Biophys. Biomol. Struct. 22 (1993) 191.
[5] C.A. Hassig, S.L. Schreiber, Curr. Opin. Chem. Biol. 1 (1997) 300.
[6] Q. Wang, Y. Zhang, C. Yang, H. Xiong, Y. Lin, J. Yao, H. Li, L. Xie, W. Zhao, Y. Yao, Z.-B. Ning, R. Zeng, Y. Xiong, K.-L. Guan, S. Zhao, G.-P. Zhao, Science 327 (2010) 1004.
[7] S. Zhao, W. Xu, W. Jiang, W. Yu, Y. Lin, T. Zhang, J. Yao, L. Zhou, Y. Zeng, H. Li, Y. Li, J. Shi, W. An, S.M. Hancock, F. He, L. Qin, J. Chin, P. Yang, X. Chen, Q. Lei, Y. Xiong, K.-L. Guan, Science 327 (2010) 1000.
[8] S. Hammes-Schiffer, S.J. Benkovic, Annu. Rev. Biochem. 75 (2006) 519.
[9] I. Bahar, C. Chennubhotla, D. Tobi, Curr. Opin. Struct. Biol. 17 (2007) 633.
[10] K. Henzler-Wildman, D. Kern, Nature 450 (2007) 964.
[11] B. Eckert, A. Martin, J. Balbach, F.X. Schmid, Nat. Struct. Mol. Biol. 12 (2005) 619.
[12] A. Ansari, J. Berendzen, S.F. Bowne, H. Frauenfelder, I.E.T. Iben, T.B. Sauke, E. Shyamsunder, R.D. Young, Proc. Natl. Acad. Sci. U.S.A. 82 (1985) 5000.
[13] J.D. Bryngelson, J.N. Onuchic, N.D. Socci, P.G. Wolynes, Proteins: Struct. Funct. Genet. 21 (1995) 167.
[14] D. Kern, E.R.P. Zuiderweg, Curr. Opin. Struct. Biol. 13 (2003) 748.
[15] S. Aono, Dalton Trans. (2008) 3137.
[16] G.R. Moore, G.W. Pettigrew, Cytochromes *c*: Evolutionary, Structural and Physicochemical Aspects, Springer-Verlag, New York, 1990.
[17] M.T. Wilson, C. Greenwood, in: R.A. Scott, A.G. Mauk (Eds.), Cytochrome *c*: A Multidisciplinary Approach, University Science Books, Sausalito, CA, 1996, p. 611.
[18] A.J. Di Bilio, C. Dennison, H.B. Gray, B.E. Ramirez, A.G. Sykes, J.R. Winkler, J. Am. Chem. Soc. 120 (1998) 7551.
[19] I. Moura, S.R. Pauleta, J.J.G. Moura, J. Biol. Inorg. Chem. 13 (2008) 1185.
[20] V.L. Davidson, Acc. Chem. Res. 33 (2000) 87.
[21] V.L. Davidson, Acc. Chem. Res. 41 (2008) 730.
[22] V.L. Davidson, Biochemistry 41 (2002) 14633.
[23] C. Greenwood, G. Palmer, J. Biol. Chem. 240 (1965) 3660.
[24] M.T. Wilson, C. Greenwood, Eur. J. Biochem. 22 (1971) 11.
[25] H.L. Hodges, R.A. Holwerda, H.B. Gray, J. Am. Chem. Soc. 96 (1974) 3132.
[26] P.A. Williams, V. Fulop, E.F. Garman, N.F.W. Saunders, S.J. Ferguson, J. Hajdu, Nature 389 (1997) 406.
[27] G.W. Pettigrew, G.R. Moore, Cytochromes *c*: Biological Aspects, Springer-Verlag, New York, 1987.
[28] R.E. Dickerson, R. Timkovich, in: P.D. Boyer (Ed.), The Enzymes, 3rd ed., Academic Press, New York, 1975, p. 397.
[29] Y.P. Ow, D.R. Green, Z. Hao, T.W. Mak, Nat. Rev. Mol. Cell Biol. 9 (2008) 532.
[30] C.J. Nelson, M.J. LaConte, B.E. Bowler, J. Am. Chem. Soc. 123 (2001) 7453.
[31] L. Hoang, H. Maity, M.M. Krishna, Y. Lin, S.W. Englander, J. Mol. Biol. 331 (2003) 37.
[32] M.M. Krishna, Y. Lin, J.N. Rumbley, S.W. Englander, J. Mol. Biol. 331 (2003) 29.
[33] Y. Bai, T.R. Sosnick, L. Mayne, S.W. Englander, Science 269 (1995) 192.
[34] S. Godbole, A. Dong, K. Garbin, B.E. Bowler, Biochemistry 36 (1997) 119.
[35] S. Godbole, B.E. Bowler, Biochemistry 38 (1999) 487.
[36] C.J. Nelson, B.E. Bowler, Biochemistry 39 (2000) 13584.
[37] C. Weber, B. Michel, H.R. Bosshard, Proc. Natl. Acad. Sci. U.S.A. 84 (1987) 6687.
[38] S. Döpner, P. Hildebrandt, F.I. Rosell, A.G. Mauk, J. Am. Chem. Soc. 120 (1998) 11246.
[39] S. Döpner, P. Hildebrandt, F.I. Rosell, A.G. Mauk, M. von Walter, G. Buse, T. Soulimane, Eur. J. Biochem. 261 (1999) 379.
[40] M. Assfalg, I. Bertini, A. Dolfi, P. Turano, A.G. Mauk, F.I. Rosell, H.B. Gray, J. Am. Chem. Soc. 125 (2003) 2913.
[41] R. Jemmerson, J. Liu, D. Hausauer, K.P. Lam, A. Mondino, R.D. Nelson, Biochemistry 38 (1999) 3599.
[42] A.M. Berghuis, G.D. Brayer, J. Mol. Biol. 223 (1992) 959.
[43] L.J.C. Jeuken, Biochim. Biophys. Acta 1604 (2003) 67.
[44] A. Avila, B.W. Gregory, K. Niki, T.M. Cotton, J. Phys. Chem. B 104 (2000) 2759.
[45] Q. Chi, O. Farver, J. Ulstrup, Proc. Natl. Acad. Sci. U.S.A. 102 (2005) 16203.
[46] S.W. Englander, L. Mayne, Y. Bai, T.R. Sosnick, Protein Sci. 6 (1997) 1101.
[47] S.W. Englander, Annu. Rev. Biophys. Biomol. Struct. 29 (2000) 213.
[48] S.W. Englander, L. Mayne, J.N. Rumbley, Biophys. Chem. 101–102 (2002) 57.
[49] Y. Bai, J.S. Milne, L. Mayne, S.W. Englander, Proteins 17 (1993) 75.
[50] J.M. Scholtz, G.R. Grimsley, C.N. Pace, Methods Enzymol. 466 (2009) 549.
[51] J.A. Schellman, Biopolymers 17 (1978) 1305.
[52] J.K. Myers, C.N. Pace, J.M. Scholtz, Protein Sci. 4 (1995) 2138.
[53] M.M. Krishna, H. Maity, J.N. Rumbley, Y. Lin, S.W. Englander, J. Mol. Biol. 359 (2006) 1410.
[54] Y. Xu, L. Mayne, S.W. Englander, Nat. Struct. Biol. 5 (1998) 774.
[55] H. Maity, M. Maity, S.W. Englander, J. Mol. Biol. 343 (2004) 223.
[56] H. Maity, M. Maity, M.M. Krishna, L. Mayne, S.W. Englander, Proc. Natl. Acad. Sci. U.S.A. 102 (2005) 4741.
[57] R. Kristinsson, B.E. Bowler, Biochemistry 44 (2005) 2349.
[58] M.G. Duncan, M.D. Williams, B.E. Bowler, Protein Sci. 18 (2009) 1155.
[59] P. Weinkam, C.H. Zong, P.G. Wolynes, Proc. Natl. Acad. Sci. U.S.A. 102 (2005) 12401.
[60] M.M.G. Krishna, H. Maity, J.N. Rumbley, S.W. Englander, Protein Sci. 16 (2007) 1946.
[61] A. Borgia, D. Bonivento, C. Travaglini-Allocatelli, A. Di Matteo, M. Brunori, J. Biol. Chem. 281 (2006) 9331.
[62] S. Gianni, C. Travaglini-Allocatelli, F. Cutruzzola, M. Brunori, M.C.R. Shastry, H. Roder, J. Mol. Biol. 330 (2003) 1145.
[63] E.V. Pletneva, H.B. Gray, J.R. Winkler, Proc. Natl. Acad. Sci. U.S.A. 102 (2005) 18397.
[64] M.C.R. Shastry, H. Roder, Nat. Struct. Biol. 5 (1998) 385.
[65] S. Godbole, B. Hammack, B.E. Bowler, J. Mol. Biol. 296 (2000) 217.
[66] L.V. Michel, K.L. Bren, J. Biol. Inorg. Chem. 13 (2008) 837.
[67] N. Osheroff, D. Borden, W.H. Koppenol, E. Margoliash, J. Biol. Chem. 255 (1980) 1689.
[68] F.I. Rosell, J.C. Ferrer, A.G. Mauk, J. Am. Chem. Soc. 120 (1998) 11234.
[69] J.C. Ferrer, J.G. Guillemette, R. Bogumil, S.C. Inglis, M. Smith, A.G. Mauk, J. Am. Chem. Soc. 115 (1993) 7507.
[70] W.B.R. Pollock, F.I. Rosell, M.B. Twitchett, M.E. Dumont, A.G. Mauk, Biochemistry 37 (1998) 6124.
[71] H. Maity, J.N. Rumbley, S.W. Englander, Proteins 63 (2006) 349.
[72] W.A. Eaton, R.M. Hochstrasser, J. Chem. Phys. 46 (1967) 2533.

[73] I. Dragomir, A. Hagarman, C. Wallace, R. Schweitzer-Stenner, Biophys. J. 92 (2007) 989.
[74] N. Sutin, J.K. Yandell, J. Biol. Chem. 247 (1972) 6932.
[75] P.A. Adams, D.A. Baldwin, H.M. Marques, in: A.G. Mauk, R.A. Scott (Eds.), Cytochrome *c*: A Multidisciplinary Approach, University Science Books, Sausalito, CA, 1996, p. 635.
[76] S. Baddam, B.E. Bowler, Biochemistry 44 (2005) 14956.
[77] S. Bandi, S. Baddam, B.E. Bowler, Biochemistry 46 (2007) 10643.
[78] B.K. Hawkins, S. Hilgen-Willis, G.J. Pielak, J.H. Dawson, J. Am. Chem. Soc. 116 (1994) 3111.
[79] B.A. Feinberg, X. Liu, M.D. Ryan, A. Schejter, C.Y. Zhang, E. Margoliash, Biochemistry 37 (1998) 13091.
[80] B.S. Russell, R. Melenkivitz, K.L. Bren, Proc. Natl. Acad. Sci. U.S.A. 97 (2000) 8312.
[81] B.S. Russell, K.L. Bren, J. Biol. Inorg. Chem. 7 (2002) 909.
[82] B.E. Bowler, K. May, T. Zaragoza, P. York, A. Dong, W.S. Caughey, Biochemistry 32 (1993) 183.
[83] S. Baddam, B.E. Bowler, Biochemistry 45 (2006) 4611.
[84] D.R. Hickey, A.M. Berghuis, G. Lafond, J.A. Jaeger, T.S. Cardillo, D. McLendon, G. Das, F. Sherman, G.D. Brayer, G. McLendon, J. Biol. Chem. 266 (1991) 11686.
[85] B.T. Nall, E.H. Zuniga, T.B. White, L.C. Wood, L. Ramdas, Biochemistry 28 (1989) 9834.
[86] K.M. Black, C.J.A. Wallace, Biochem. Cell Biol. 85 (2007) 366.
[87] L.L. Pearce, A.L. Gartner, M. Smith, A.G. Mauk, Biochemistry 28 (1989) 3152.
[88] W.J. Becktel, J.A. Schellman, Biopolymers 26 (1987) 1859.
[89] L.M. Herrmann, B.E. Bowler, Protein Sci. 6 (1997) 657.
[90] L.A. Davis, A. Schejter, G.P. Hess, J. Biol. Chem. 249 (1974) 2624.
[91] G. Battistuzzi, M. Borsari, F. De Rienzo, G. Di Rocco, A. Ranieri, M. Sola, Biochemistry 46 (2007) 1694.
[92] R.E. Martinez, B.E. Bowler, J. Am. Chem. Soc. 126 (2004) 6751.
[93] H. Hasumi, Biochim. Biophys. Acta 626 (1980) 265.
[94] E. Stellwagen, J. Babul, H. Wilgus, Biochim. Biophys. Acta 405 (1975) 115.
[95] G.W. Pettigrew, I. Aviram, A. Schejter, Biochem. Biophys. Res. Commun. 68 (1976) 807.
[96] G.G. Silkstone, C.E. Cooper, D. Svistunenko, M.T. Wilson, J. Am. Chem. Soc. 127 (2005) 92.
[97] F.I. Rosell, T.R. Harris, D.P. Hildebrand, S. Döpner, P. Hildebrandt, A.G. Mauk, Biochemistry 39 (2000) 9047.
[98] P.M.A. Gadsby, J. Peterson, N. Foote, C. Greenwood, A.J. Thomson, Biochem. J. 246 (1987) 43.
[99] R.T. Hartshorn, G.R. Moore, Biochem. J. 258 (1989) 595.
[100] P. Tonge, G.R. Moore, C.W. Wharton, Biochem. J. 258 (1989) 599.
[101] P. Weinkam, J. Zimmermann, L.B. Sagle, S. Matsuda, P.E. Dawson, P.G. Wolynes, F.E. Romesberg, Biochemistry 47 (2008) 13470.
[102] H. Kihara, S. Saigo, H. Nakatani, K. Hiromi, M. Ikeda-Saito, T. Iizuka, Biochim. Biophys. Acta 430 (1976) 225.
[103] D. Verbaro, A. Hagarman, J. Soffer, R. Schweitzer-Stenner, Biochemistry 48 (2009) 2990.
[104] S. Saigo, J. Biochem. 89 (1981) 1977.
[105] T. Uno, Y. Nishimura, M. Tsuboi, Biochemistry 23 (1984) 6802.
[106] R. Shah, R. Schweitzer-Stenner, Biochemistry 47 (2008) 5250.
[107] X. Hong, D.W. Dixon, FEBS Lett. 246 (1989) 105.
[108] J.S. Redzic, B.E. Bowler, Biochemistry 44 (2005) 2900.
[109] E. Wandschneider, B.N. Hammack, B.E. Bowler, Biochemistry 42 (2003) 10659.
[110] B.T. Nall, in: R.A. Scott, A.G. Mauk (Eds.), Cytochrome *c*: A Multidisciplinary Approach, University Science Books, Sausalito, CA, 1996, p. 167.
[111] L.C. Wood, T.B. White, L. Ramdas, B.T. Nall, Biochemistry 27 (1988) 8562.
[112] M.M. Pierce, B.T. Nall, Protein Sci. 6 (1997) 618.
[113] B.M. Hoffman, M.A. Ratner, J. Am. Chem. Soc. 109 (1987) 6237.
[114] B.M. Hoffman, M.A. Ratner, S.A. Wallin, Adv. Chem. Ser. 226 (1990) 125.
[115] B.S. Brunschwig, N. Sutin, J. Am. Chem. Soc. 111 (1989) 7454.
[116] N. Sutin, B.S. Brunschwig, Adv. Chem. Ser. 226 (1990) 65.
[117] D.B. Rorabacher, N.E. Meagher, K.L. Juntunen, P.V. Robandt, G.H. Leggett, C.A. Salhi, B.C. Dunn, R.R. Schroeder, L.A. Ochrymowycz, Pure Appl. Chem. 65 (1993) 573.
[118] P. Rosen, I. Pecht, Biochemistry 15 (1976) 775.
[119] A.G. Lappin, C.A. Lewis, W.J. Ingledew, Inorg. Chem. 24 (1985) 1446.
[120] M.M. Ivković-Jensen, N.M. Kostić, Biochemistry 36 (1997) 8135.
[121] H. Mei, K. Wang, N. Peffer, G. Weatherly, D.S. Cohen, M. Miller, G. Pielak, B. Durham, F. Millett, Biochemistry 38 (1999) 6846.
[122] W.B. Davis, M.A. Ratner, M.R. Wasielewski, J. Am. Chem. Soc. 123 (2001) 7877.
[123] R.C. Lasey, L. Liu, L. Zang, M.Y. Ogawa, Biochemistry 42 (2003) 3904.
[124] L. Liu, J. Hong, M.Y. Ogawa, J. Am. Chem. Soc. 126 (2004) 50.
[125] J.L. Blazyk, G.T. Gassner, S.J. Lippard, J. Am. Chem. Soc. 127 (2005) 17364.
[126] B.M. Hoffman, L.M. Celis, D.A. Cull, A.D. Patel, J.L. Seifert, K.E. Wheeler, J. Wang, J. Yao, I.V. Kurnikov, J.M. Nocek, Proc. Natl. Acad. Sci. U.S.A. 102 (2005) 3564.
[127] N.E. Meagher, K.L. Juntunen, C.A. Salhi, L.A. Ochrymowycz, D.B. Rorabacher, J. Am. Chem. Soc. 114 (1992) 10411.
[128] P. Wijetunge, C.P. Kulatilleke, L.T. Dressel, M.J. Heeg, L.A. Ochrymowycz, D.B. Rorabacher, Inorg. Chem. 39 (2000) 2897.
[129] D.B. Rorabacher, Chem. Rev. 104 (2004) 651.
[130] M.J. Martin, J.F. Endicott, L.A. Ochrymowycz, D.B. Rorabacher, Inorg. Chem. 26 (1987) 3012.
[131] G.H. Leggett, B.C. Dunn, A.M.Q. Vande Linde, L.A. Ochrymowycz, D.B. Rorabacher, Inorg. Chem. 32 (1993) 5911.
[132] Q. Yu, C.A. Salhi, E.A. Ambundo, M.J. Heeg, L.A. Ochrymowycz, D.B. Rorabacher, J. Am. Chem. Soc. 123 (2001) 5720.
[133] E.A. Ambundo, L.A. Ochrymowycz, D.B. Rorabacher, Inorg. Chem. 40 (2001) 5133.
[134] E.A. Ambundo, Q. Yu, L.A. Ochrymowycz, D.B. Rorabacher, Inorg. Chem. 42 (2003) 5267.
[135] P.D. Barker, A.G. Mauk, J. Am. Chem. Soc. 114 (1992) 3619.
[136] A.L. Raphael, H.B. Gray, J. Am. Chem. Soc. 113 (1991) 1038.
[137] S. Wherland, H.B. Gray, in: A.W. Addison, W.R. Cullen, D. Dolphin, B.R. James (Eds.), Biological Aspects of Inorganic Chemistry, Wiley Interscience, New York, NY, 1977, p. 289.
[138] S. Baddam, B.E. Bowler, J. Am. Chem. Soc. 127 (2005) 9702.
[139] S. Baddam, B.E. Bowler, Inorg. Chem. 45 (2006) 6338.
[140] S. Bandi, B.E. Bowler, J. Am. Chem. Soc. 130 (2008) 7540.
[141] B.E. Bowler, A.L. Raphael, H.B. Gray, Prog. Inorg. Chem. 38 (1990) 259.
[142] M.A. Cusanovich, G. Tollin, in: R.A. Scott, A.G. Mauk (Eds.), Cytochrome *c*: A Multidisciplinary Approach, University Science Books, Sausalito, CA, 1996, p. 489.
[143] A.J. Ahmed, F. Millett, J. Biol. Chem. 256 (1981) 1611.
[144] J. Butler, D.M. Davies, A.G. Sykes, W.H. Koppenol, N. Osheroff, E. Margoliash, J. Am. Chem. Soc. 103 (1981) 469.
[145] J. Butler, S.K. Chapman, D.M. Davies, A.G. Sykes, S.H. Speck, N. Osheroff, E. Margoliash, J. Biol. Chem. 258 (1983) 6400.
[146] P.L. Drake, R.T. Hartshorn, J. McGinnis, A.G. Sykes, Inorg. Chem. 28 (1989) 1361.
[147] S. Speh, H. Elias, J. Biol. Chem. 269 (1994) 6370.
[148] G. Cheddar, T.E. Meyer, M.A. Cusanovich, C.D. Stout, G. Tollin, Biochemistry 28 (1989) 6318.
[149] E. Margoliash, H.R. Bosshard, Trends Biochem. Sci. 8 (1983) 316.
[150] W.H. Koppenol, E. Margoliash, J. Biol. Chem. 257 (1982) 4426.
[151] S. D'Amico, J.C. Marx, C. Gerday, G. Feller, J. Biol. Chem. 278 (2003) 7891.
[152] J. Hollien, S. Marqusee, Proc. Natl. Acad. Sci. U.S.A. 96 (1999) 13674.